VOLUME 2 NUMBER 4 2009

TRANSACTIONS ON TRANSPORT SCIENCES

Ministry of Transport

CZECH TECHNICAL UNIVERSITY

TRANSACTIONS ON TRANSPORT SCIENCES

Publisher: *Ministry of Transport*, nábř. L. Svobody 1222/12, 110 15 Praha 1, Czech Republic
E-mail: *info@transportsciences.org*
URL: *www.transportsciences.org*

Editorial Office: Olga Krištofíková
Hedvika Kovandová
Jana Zelinková
Vladimír Adamec
Petr Polanský
Irena Zedková

Periodicity: Quarterly
Language: English
Scope: International scientific journal for transport sciences
Print version: ISSN 1802-971X
On-line version: ISSN 1802-9876
Registration Number: MK EČ E 18012

Each paper in the journal is evaluated by two reviewers under the supervision of the International Editorial Board.

The Research and Development Council of the Government of the Czech Republic indexed this journal in the Title List of Peer-Reviewed Journals.

Distributor: CDV – Transport Research Centre, Líšeňká 33a, 636 00 Brno, Czech Republic,
journal@cdv.cz

Influence of Periodic Freezing on the Value of the Elastic Modulus of Light-weight Fibre Concrete

O. Pospíchal*, B. Kucharczyková, P. Misák, Z. Hlaváč, T. Vymazal
Institute of Building Testing, Faculty of Civil Engineering, Brno University of Technology, Brno, Czech Republic
** Corresponding author: pospichal.o@fce.vutbr.cz*

ABSTRACT: This paper deals with the influence of periodic freezing on light-weight concrete characteristics. Three different sets of light-weight concrete specimens were periodically freezing and non-destructively tested over time. Another three comparative sets of light-weight concrete specimens were tested at the same time and these sets were placed in water. The main aim was to determine and compare the dynamic elastic modulus values during and after 200 freeze-thaw cycles. The methods for this non-destructive testing were the ultrasonic impulse method and the resonance method.

KEY WORDS: Light-weight concrete, freeze-thaw resistance, ultrasonic impulse method, resonance method.

1 INTRODUCTION

The freeze-thaw resistance of concrete is related to its air void system and to the bond between the aggregates and matrix. Light-weight aggregate concretes are characterized by specific distribution and the content of air voids in the matrix as well as in the aggregate particles. The main disadvantage of these concretes is their high sensitivity to the curing conditions which can significantly influence the initiation and propagation of cracks. This fact leads to the changes of physical-mechanical, fracture, and durability parameters. One of the approaches to controlling the propagation of cracks is the application of various types of fibre reinforcement in a variety of amounts.

This paper deals with a part of the results of the experimental analysis focused on the freeze-thaw resistance of the light-weight concrete. Polypropylene fibres Forta Econo Net with a length of 38 mm and 19 mm were used as a dispersed reinforcement.

2 COMPOSITION OF LIGHT-WEIGHT CONCRETE

Fresh concrete mixture was prepared from Liapor 4–8/600 light-weight aggregates (year of delivery 2006), heavy-weight aggregates (DTK) of 0–4 mm fraction, CEM I – 42.5 R cement, fly ash, plasticizer and water. The water and light-weight aggregates of 4–8 mm fraction were dosed by volume, the remaining components by weight. Three mixtures were made: REF, EN38 and EN19. Mixture REF was made without fibres, mixture EN38

and EN19 differed only in the type of fibres used. The dosage of both was 0.9 kg/m3. The composition of the fresh concrete mixture is given in Table 1; workability – flow test – was F4 for all prepared mixtures REF, EN38 and EN19.

Table 1: Composition of fresh concrete mixture

Components	Units	Quantities per 1 m3
Liapor 4–8/600	m3	0.44
DTK 0–4 mm Bratčice	kg/m3	580
Cement 42.5 R	kg/m3	400
Fly ash Třinec	kg/m3	50.0
Plasticizer Sika Viscocrete 1035	kg/m3	5.00
Water	l	206

3 FREEZE-THAW TEST

The cyclical freezing and thawing of the saturated concrete specimens is the basic testing method for the determination of concrete freeze-thaw resistance (ČSN 73 1322). According to the Czech standard the basic results of this test are, especially, decreases in mass, bending strengths, compressive strengths on the prism's fragments, coefficient of freeze-thaw resistance, and changes of monitored parameters measured with the dynamic NDT method within particular periods. These parameters are mainly used for the determination of the rate of the internal structural damage.

For the experimental analysis two sets of prismatic specimens were used. The first set was exposed to the cyclical freezing and thawing (4 hours freezing and 2 hours thawing). The second set was not frost-attacked (specimens were only immersed in water). Each set contained three different types of LWAC – REF (concrete without fibres), EN38 (concrete with fibres Forta Econo Net 38 mm), and EN19 (concrete with fibres Forta Econo Net 19 mm). All sets were tested at the same age after which the first set had achieved 200 freeze-thaw cycles.

4 EXPERIMENTAL

4.1 Testing methods

The ultrasonic impulse method is widely used for non-destructive determination of the quality of concrete. The method is based on the measurement of the transmission time of an ultrasonic impulse through the tested material. The method is useful in providing information about the uniformity of the concrete, cavities, cracks and defects, the modulus of elasticity, and compressive strength.

The resonance method is intended primarily for detecting significant changes in the dynamic modulus of the elasticity of laboratory or field test specimens that are undergoing exposure to weathering or other types of potentially detrimental influences. The test method may also be used to monitor the development of dynamic elastic modulus with increasing maturity of test specimens. This test method covers measurement of the fundamental transverse, longitudinal, and torsional resonant frequencies of concrete specimens (ASTM International).

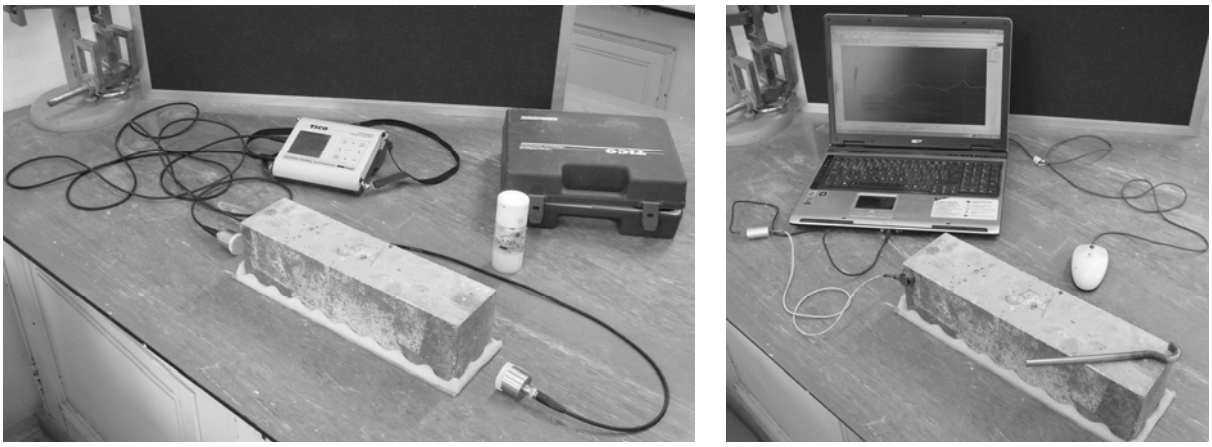

Figure1: Testing equipment – ultrasonic impulse method (left), resonance method (right)

4.2 Dynamic Modulus of Elasticity

Internal damage, which can arise during freezing, leads to changes in concrete properties. The volume of the internal damage is related to the value of the dynamic elastic modulus and, according to the Czech standard ČSN 73 1380, it is possible to use two methods to determine the relative dynamic elastic modulus of prismatic specimens. The first method is an ultrasonic impulse method whilst the second is a resonance method.

Both methods are non-destructive testing methods and it is possible to use the following equations for the determination of the relative dynamic elastic modulus:

$$RDM_{UPPT,n} = \left(\frac{t_{S,0}}{t_{S,n}} \right)^2 \times 100 \quad [\%] \,,$$

where

RDMUPPT,n is the relative dynamic modulus of elasticity evaluated from the ultrasonic impulse method;

tS,0 is the transmit time of the ultrasonic impulse in [μs] at a starting measurement;

tS,n is the transmit time of the ultrasonic impulse in [μs] at a measurement after n number of the freeze-thaw cycles.

$$RDM_{FF,n} = \left(\frac{f_n}{f_0} \right)^2 \times 100 \quad [\%] \,,$$

where

RDMFF,n is the relative dynamic modulus of elasticity evaluated from the resonance method;

fn is the fundamental transverse resonant frequency in [Hz] at a measurement after n number of the freeze-thaw cycles;

f0 is the fundamental transverse resonant frequency in [Hz] at the starting measurement.

Both the equations lead to a value that is interpreted as a percentage. It is also possible to express the results of dynamic elastic modulus in specific units according to the Czech standards; ČSN 73 1371 for the ultrasonic impulse method and ČSN 73 1372 for the resonance method.

5 EXPERIMENTAL RESULTS

Results of the experimental analysis are given in following figures which show their mean values with the standard deviations of the relative modulus of elasticity during and after the freeze-thaw test. The dimensions of the tested specimens were 400x100x100 mm. The number of specimens in each set is presented in Table 2.

Table 2: Number of specimens in each tested set

Type of concrete	Specifications	Amount of specimens
REF	non-frost-attacked	5
	frost-attacked	4
EN38	non-frost-attacked	7
	frost-attacked	6
EN19	non-frost-attacked	6
	frost-attacked	6

The following three figures show the mean values of the relative dynamic elastic modulus of the three types of the light-weight concrete. The left part of each figure represents values evaluated from the ultrasonic impulse method and the right parts of figures show the results from the resonance method. Every couple of bars in figures there is a comparison of the non-frost-attacked and the frost-attacked specimens at the same time during the cyclical freezing.

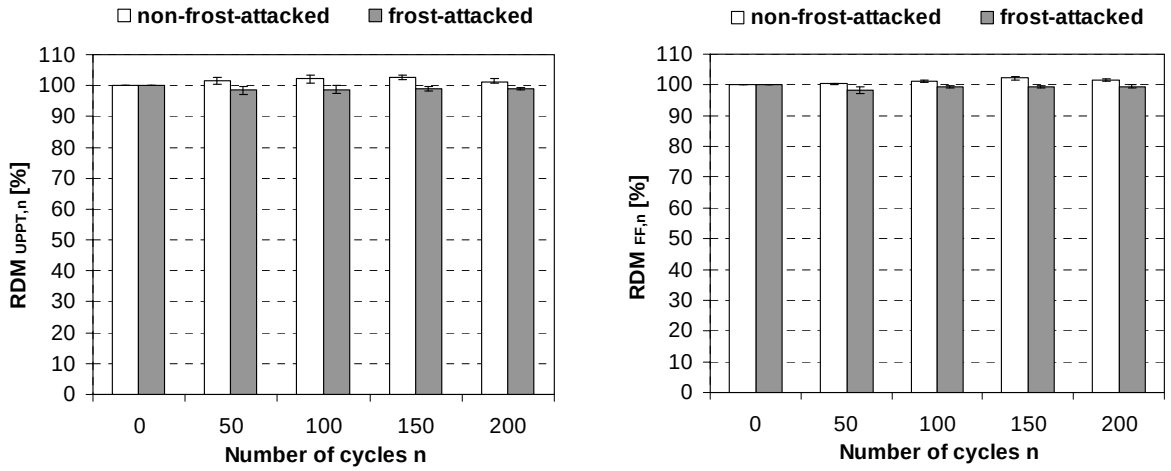

Figure 2: Relative dynamic modulus of elasticity – concrete REF.

Figure 2 presents results for the concrete REF (without fibres).

Figure 3 presents results for the concrete EN38 (concrete with fibres Forta Econo Net 38 mm).

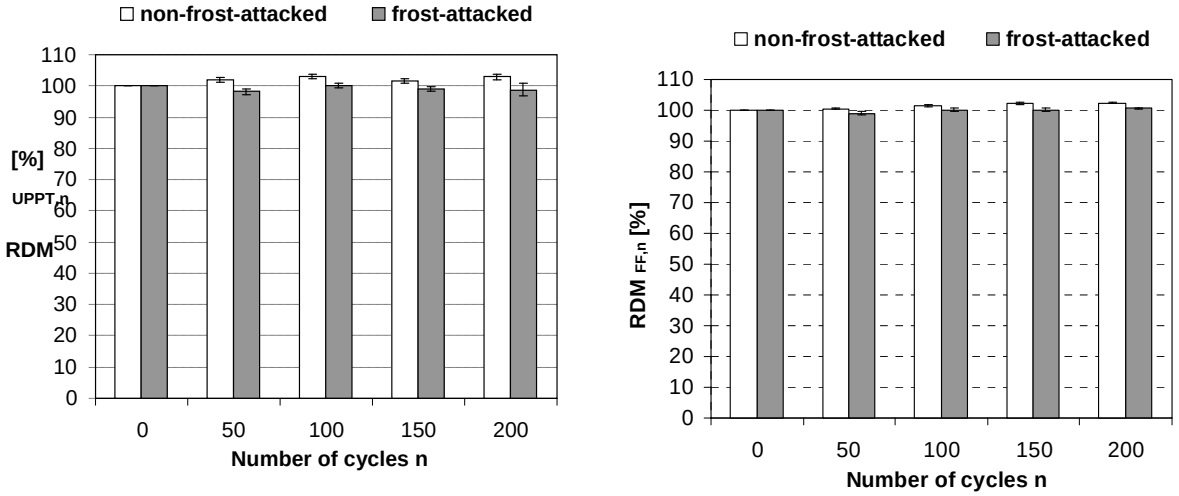

Figure 3: Relative dynamic modulus of elasticity – concrete EN38.

Figure 4 presents results for the concrete EN19 (concrete with fibres Forta Econo Net 19 mm).

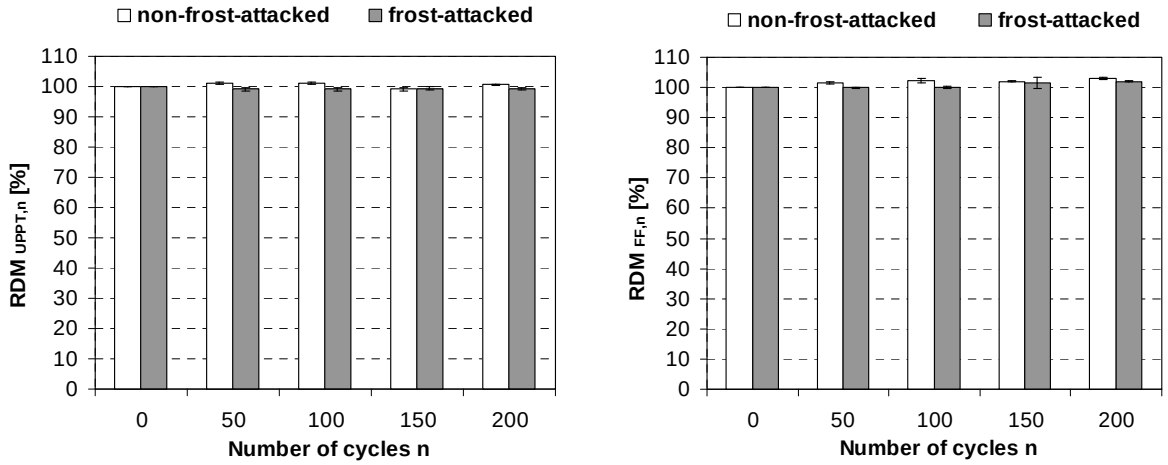

Figure 4: Relative dynamic modulus of elasticity – concrete EN19.

The following two figures show the mean values of the dynamic elastic modulus in specific units GPa of all three types of concrete after 200 freeze-thaw cycles. Figure 5 presents the values evaluated from the ultrasonic impulse method and Figure 6 from the

resonance method. Every couple of bars in the figures there is a comparison of the non-frost-attacked and the frost-attacked specimens after the cyclical freezing.

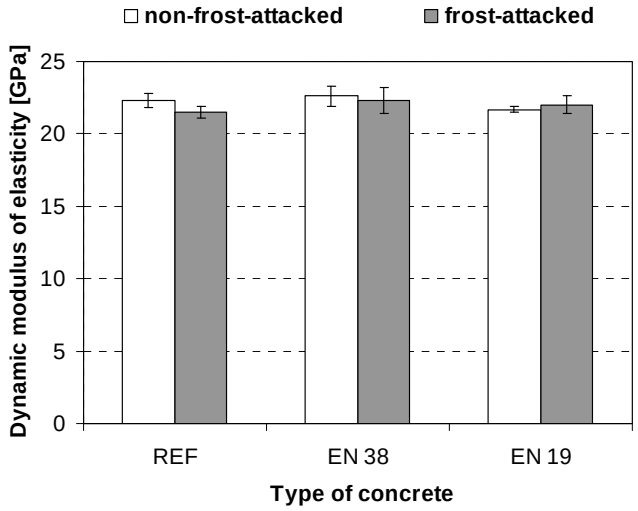

Figure 5: Dynamic modulus of elasticity in GPa evaluated from the ultrasonic impulse method for three types of concrete.

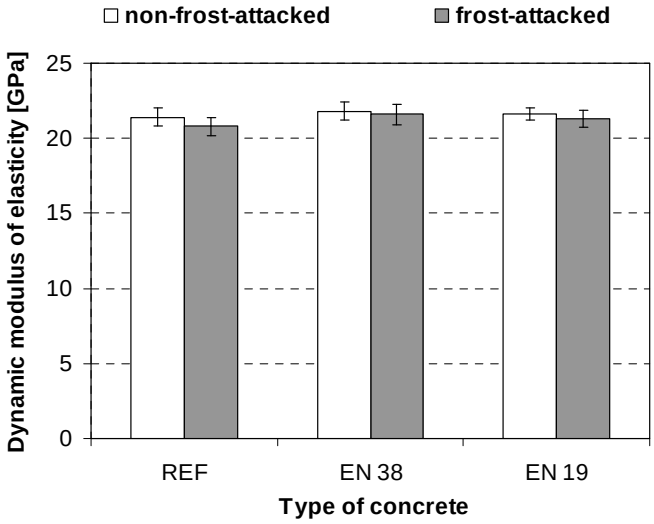

Figure 6: Dynamic modulus of elasticity in GPa evaluated from the resonance method for three types of concrete.

6 CONCLUSIONS

From the above-presented results it is possible to conclude:

- The results of both measurement methods are comparable and, unless there are markedly more defects in the structure of the tested specimens, both methods are applicable to evaluate the modulus of elasticity of concrete.

- All three tested types of concrete are of good enough quality from a freeze-thaw resistance point of view. No mechanical damage or opened cracks on the specimen's surface were observed.
- Frost-attacked specimens show slightly lower values for the modulus of elasticity. Nevertheless, the evaluated values were between 20 and 25 GPa for the frost-attacked specimens, as well as for the non-frost-attacked specimens.

From the performed experiments it is possible to draw the following ideas:

- Non-destructive testing methods – the ultrasonic impulse method and the resonance method – are useful for the evaluation of the dynamic modulus of elasticity and for the monitoring of structural changes in concrete during the freeze-thaw test.
- These methods are insufficient for the description of the total rate of damage of the internal structure in the case of high freeze-thaw resistance concrete.
- For a more detailed overview of material properties it is indispensable to apply more testing methods which are more sensitive to damage by micro-cracks, for example, the determination of the static modulus of elasticity in bending, determination of compressive strength or splitting tensile strength on the prism fragments.
- In recent years the fracture test has been used for a description of material brittleness. The fracture parameters – effective fracture toughness value, work of fracture value – complete all above-mentioned characteristics very well.

7 ACKNOWLEDGEMENT

This outcome has been achieved with the financial support of the Ministry of Education, Youth and Sports, project No. 1M06005, within the activities of the CIVAK research centre, and the Internal Grant of FCE BUT, project No. VG A52.

REFERENCES

ČSN 73 1322 Determination of the concrete freeze-thaw resistance. Czech Standards Institute, 1968.

ČSN 73 1371 Method of ultrasonic pulse testing of concrete. Czech Standards Institute, 1981.

ČSN 73 1372 Testing of concrete by resonance method. Czech Standards Institute, 1981.

ČSN 73 1380 Testing the freeze-thaw resistance of concrete – Internal structural damage. Czech Standards Institute, 2007.

Frantík, P., Keršner, Z.: Vyhodnocení lomového experimentu s katastrofickou ztrátou stability. In: Sborník mezinárodní konference Staticko-konštrukčné a stavebno-fyzikálne problémy stavebných konštrukcií, Štrbské Pleso, 2006, pp. 141–142 (in Czech).

Hlaváč, Z.; Kucharczyková, B.; Cikrle, P. Light construction Liapor concrete's freeze-thaw resistance. In Proceedings of the International Conference LC2008. Brno, 2008. p. 99 - 104. ISBN 978-80-214-3773-9.

Kucharczyková, B.; Keršner, Z. Influence of Freeze-Thaw Cycles on Fracture Behaviour of Fibre Reinforced Light-Weight Concrete Specimens. In Proceedings of 5th International Conference Concrete and Concrete Structures. Žilina, 2009. p. 133 - 138. ISBN 978-80-554-0100-3.

Veselý, V.: Concrete parameters for description of fracture behaviour. Institute of Structural Mechanics, Faculty of Civil Engineering, Brno University of Technology, Czech Republic: dissertation theses, 2004 (in Czech).

American Society for Testing and Materials (ASTM) web site: www.astm.org

Location of Steel Reinforcement and Other Reinforcing Elements using 3D GPR

T. Kordina* & Z. Kadlecová**
Brno University of Technology, Faculty of Civil Engineering, Department of Building Testing
** Corresponding author: kordina.t@fce.vutbr.cz*
*** Corresponding author: kadlecova.z@fce.vutbr.cz*

J. Štainbruch
Inset s.r.o., Czech Republic

ABSTRACT: This paper evaluates the results of the first experimental 3D GPR measurements by the DIBEKON scanner on a physical model. The objective of the series of measurements carried out was to determine the applicability of various types of antennae (800 MHz and 1600 MHz) in the detection of steel reinforcement and the influence of the measurement density on the quality of the resulting image of the environment examined.

KEY WORDS: GPR (Ground Penetrating Radar), NDT, concrete.

1 INTRODUCTION

One of the progressively developing non-destructive diagnostic methods is the method of Ground Penetrating Radar (GPR). This method was originally developed for geological applications, but, due to the technological development and market requirements, it is beginning to be applied more and more in the building industry.

Although the professional literature gives a number of examples of GPR applications from the USA, Europe and other advanced parts of the world, in the Czech Republic this method had not been used very much so far, and the only company systematically engaged in the georadar diagnostic research is the company INSET s.r.o. Under the auspices of this company, the first partial experimental measurements were carried out on a physical model simulating by its properties a building structure. The aim of the measurement was to evaluate the possibilities of using this method for the location of steel reinforcement and other anomalies, defects and failures in building structures.

2 THEORETICAL BASIS AND PRINCIPLE OF THE GPR METHOD

The GPR method works on the principle of radiating high-frequency electromagnetic pulses into the environment examined and registering their reflections within a time window. Measurement devices used for the diagnostics of structures work in the frequency range of 108 – 109 Hz. The signal propagation in the environment depends primarily on its electromagnetic properties – permittivity and conductivity. The speed

of electromagnetic pulse propagation can be determined, in a simplified way, from the following formula:

$$v = \frac{c}{\sqrt{\varepsilon_r}}, \tag{1}$$

where
v is the speed of electromagnetic signal propagation in the environment
c is the speed of propagation in the vacuum (c = 0,3 m/ns)
εr is the relative permittivity of the environment.

The electromagnetic signal attenuation α (dB/m) and the related maximum signal penetration depth H (m) are primarily dependent on the conductivity of the environment σ (S.m). For non-magnetic materials, we can calculate the attenuation coefficient using the following equation:

$$\alpha = 1,64\frac{\sigma}{\sqrt{\varepsilon}}. \tag{2}$$

For high-frequency electromagnetic pulses, the conductivity and therefore also the value of attenuation coefficient are frequency-dependent. At higher frequencies, the attenuation is greater, and the measurement depth range therefore lower.

On the boundary of two environments with a step change of electromagnetic properties, part of the signal is reflected.

The ability of the georadar method to detect non-homogeneities depends on many factors. A major role is played by the size of the anomaly, particularly in relation to the depth of its position and to the frequency of the measurement device. As a general rule, the georadar can detect objects larger than one half of the wavelength. To calculate the wavelength, we can use the following relation:

$$\lambda = \frac{v}{f}, \tag{3}$$

where
λ is the wavelength
v is the speed of electromagnetic signal propagation in the environment
f is the average frequency of the emitted signal.

Devices working with higher frequency antennae therefore have a greater resolving power, but their disadvantage is a smaller depth range. The sensitivity of the measurement is similarly dependent on the ratio between the useful signal and the noise, i.e., on the "tuning in" of the system, intensity of the surrounding interference (electromagnetic smog), etc.

3 DESCRIPTION OF THE MEASUREMENT

All experimental measurements on the physical model were carried out in the Prague premises of the INSET s.r.o. company, which provided sufficient background for executing research activities.

The measurements proceeded according to the agreed scenario to obtain the greatest possible amount of data from one measurement system for detailed processing. Two different types of GPR antennae were used for measurements - with transmission frequencies of 800 MHz and 1600 MHz.

3.1 Instrumentation

The measurement was carried out by means of the RAMAC GPR radar system manufactured by Swedish Malå GeoScience. The system used was a RAMAC X3M Corder in combination with shielded antennae with a medium transmission frequency of 800 MHz with a real depth range of 0.6 – 0.8 m and further the RAMAC CX system with a shielded 1600 MHz antenna with a depth range of approx. 0.3 m.

To achieve the required precision of the measurement grid of georadar scanning of the measured points in the entire area of the physical model, the company INSET s.r.o. developed a solid measuring frame with a controlled moving slider for the attachment of the georadar antenna with a working name of DIBEKON (Diagnostika betonových konstrukcí - Diagnostics of concrete structures, see Figure 1).

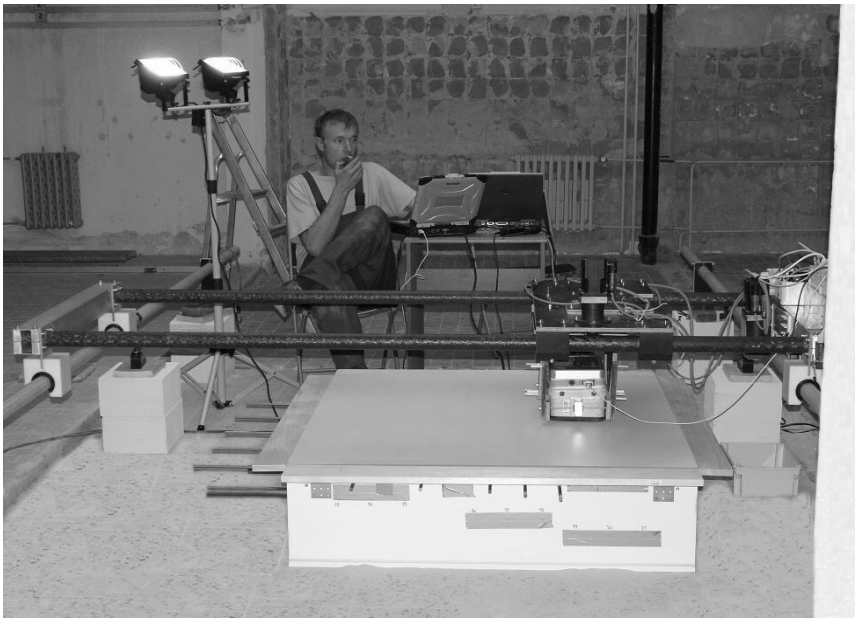

Figure1: RAMAC measuring device with a system of 800 MHz antennae attached to the DIBEKON scanning frame.

The measuring sys-tem was operated and set up and data collected by means of Ramac Ground Vision software v.1.4.5.

3.2 Physical model

To simulate a real concrete structure, a physical model was designed: the "measuring box" with external dimensions of 1200 x 1200 x 300 mm and with the familiar geometry of holes in the walls for the attachment of the diagnosed non-homogeneities. The geometry of holes was designed in order to simulate various sections of concrete reinforcement placed in the formwork (Ø 8, 10, 12 mm), ducts for the prestressing reinforcement, or other elements (Ø 30, 50, 100 mm) in the required vertical and horizontal position. In order to achieve the adequate environment equivalent to a real concrete structure, the whole space was filled with super fine silica sand after placing the concrete reinforcement. The measuring polygon

prepared in this way was covered with a fibreboard, from the upper surface of which the coverage of the steel reinforcement was measured.

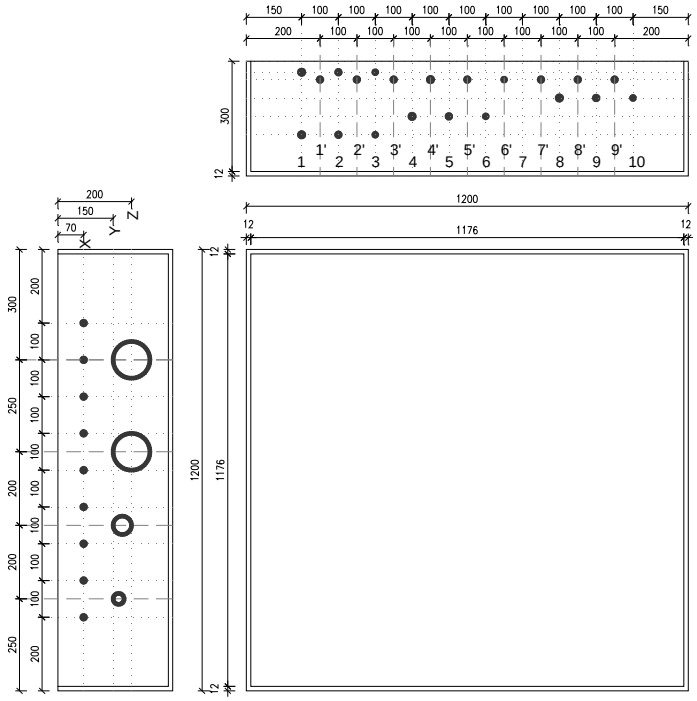

Figure 2: Diagram of the physical model.

3.3 Measurement procedure

Before the actual start of the work with GPR it was important to select the optimum arrangement of steel reinforcement in the physical model. In the first partial measurement, the concrete reinforcement bars Ø 10 mm were arranged in the X direction at distances of 200 mm with 45 mm coverage (green). Further, steel tubes Ø 30 were placed in the X direction (one free, the second one in a plastic sleeve - blue). In the Y direction, the arrangement of bars Ø 10 mm at distances of 100 mm and 200 mm was combined with 65 mm coverage (red). A control steel plate of 200 x 300 x 5 mm (grey) was placed in the formwork as the last component. For illustration see Figure 3.

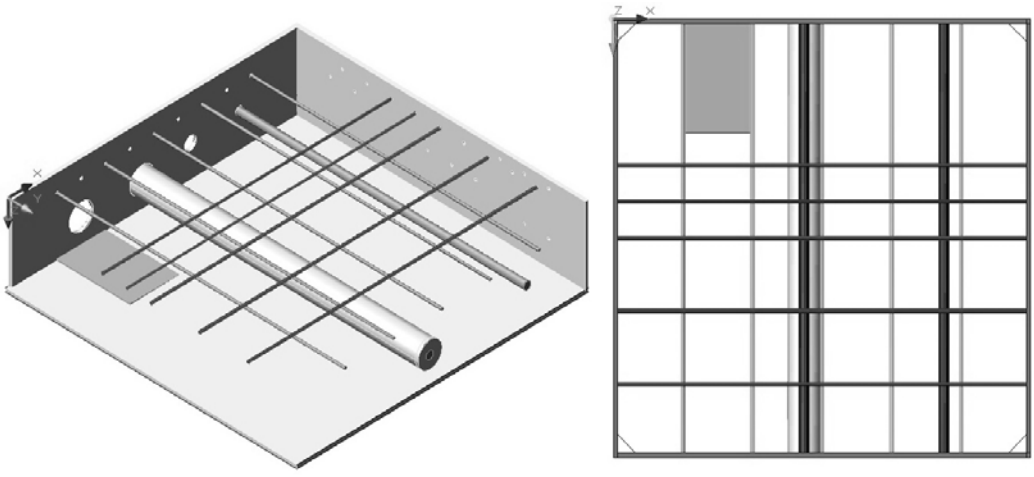

Figure 3: Arrangement of reinforcement in the physical model.

Radar measurements were carried out in the grid of measurement points given by the constant of the shift of the measuring probe along the section (in the range of 5 – 20 mm), and by the distance of the adjacent parallel sections (range 5 – 20 mm). These parameters determined the density of measurement points.

The following table shows the basic settings for individual antenna devices used.

Table 1: Basic parameters of the setting

PARAMETERS	800 MHz	1600 MHz
Antena Separation	0.140	0.060
Frequency	10129.557034	20962.778491
Frequency Steps	45	21
Stacks	8	16
Trace	26362	27900

4 DATA PROCESSING

4.1 Method of data processing

In the course of measurement, the data are recorded in the memory of the measuring computer and continuously displayed on its monitor, Figure 4 and Figure 5. This display serves chiefly as a control of system functionality. The actual evaluation of the measured data is carried out only after finishing the work on the desktop computer, by means of a special processing and graphic software (Dibekon). The measured data were processed by the ReflexW software (K.J. Sandmeier) using one- and two-dimensional filters and other mathematical operations into the shape of radar time-sections and planes.

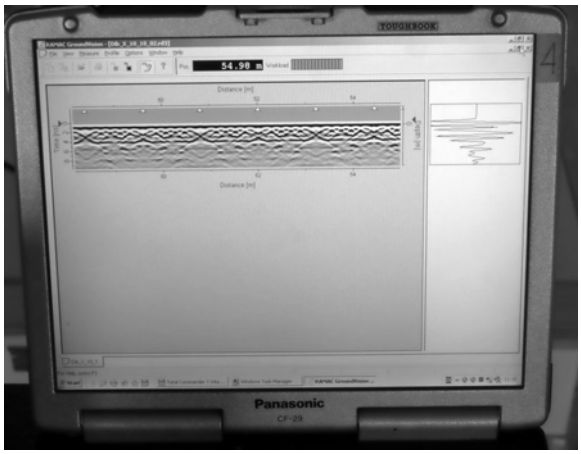

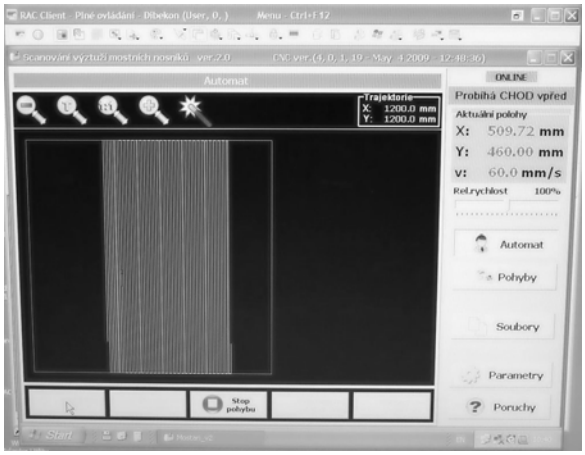

Figure4: Recording of the measurements in-situ . **Figure 5: Dibekon control unit.**

4.2 Values measured

The output of the planar measurements is a set of radar time sections for individual parallel reinforcement sections. In these sections, the individual measured traces - recordings of the amplitude changes of the reflected signal detected in time (vertical axis) - are arranged next to each other in the horizontal axis. Due to dense measurement steps, the resulting

sections represent an almost continuous image of the investigated environment. At first, the sections are processed and evaluated separately by means of mathematical filtrations and operations. The processed and adjusted sections are subsequently made into a 3D file enabling a 3D processing and visualization of the results - construction of planar sections and block diagrams.

In the graphic evaluation it is necessary to distinguish the reflections of individual bars of the upper reinforcement from false anomalies at the interference of two reflections, see Figure 14.

Partial graphic outputs provide a sufficient idea about the GPR method. Figures 7-8 show the depth sections of steel bars with 53 mm coverage. Figures 9-10 show a control steel plate located at the bottom of the measuring box. These data were measured using an antenna with a transmission frequency of 1600 MHz. Figures 11-12 show the depth sections of steel bars with 53 mm coverage. Figures 13-14 show a control steel plate located at the bottom of the measuring box. These data were measured using an antenna with a transmission frequency of 800 MHz .

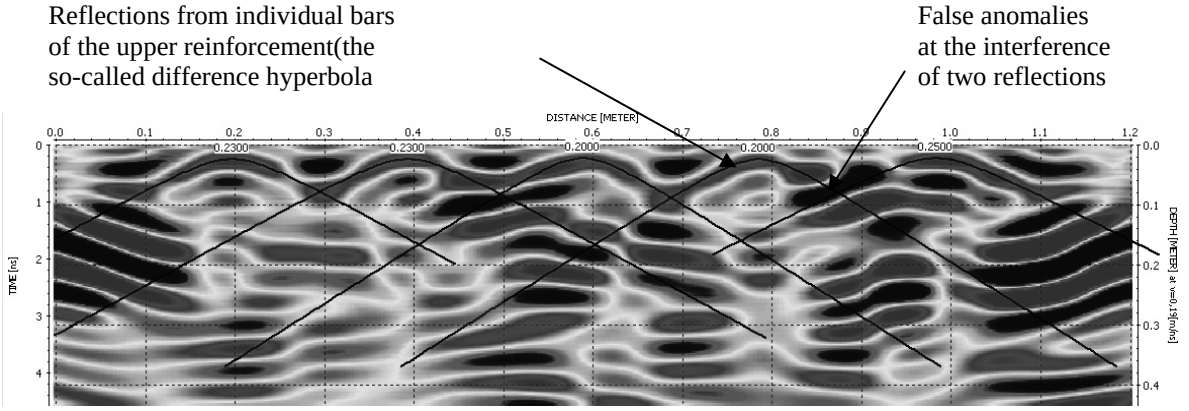

Figure 6: Longitudinal section of the radar section 1600 MHz.

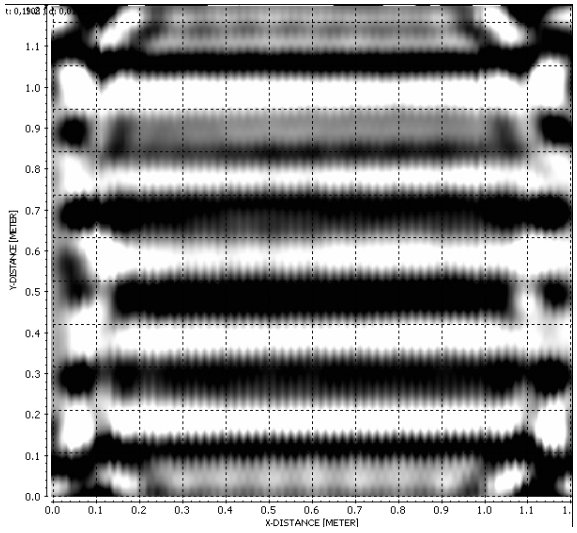

Figure 7:
Image of reinforcement in the cross direction – black and white resolution (1600 MHz).

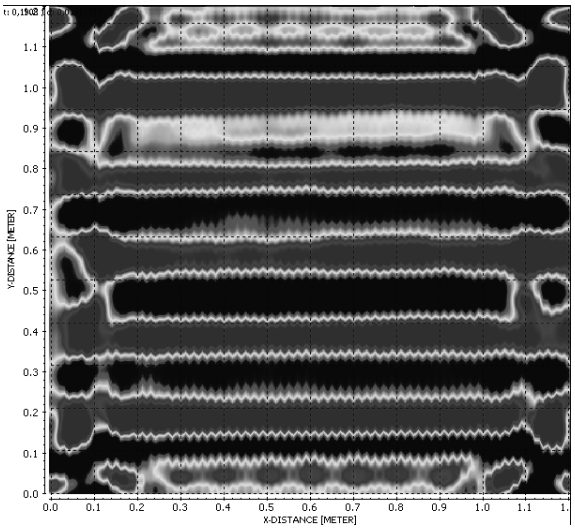

Figure 8: Image of reinforcement in the cross direction – colour resolution (1600 MHz).

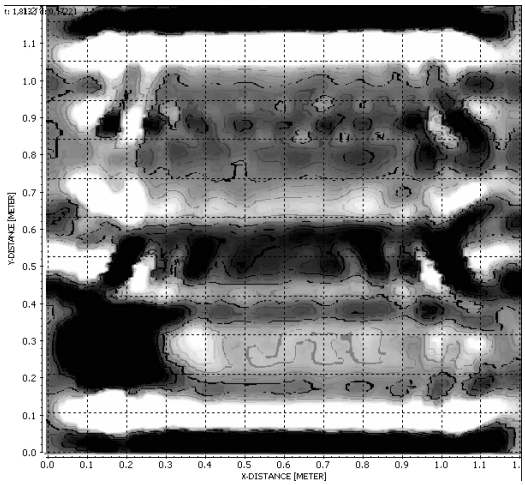

Figure 9: Image of steel plate – black and white resolution (1600 MHz).

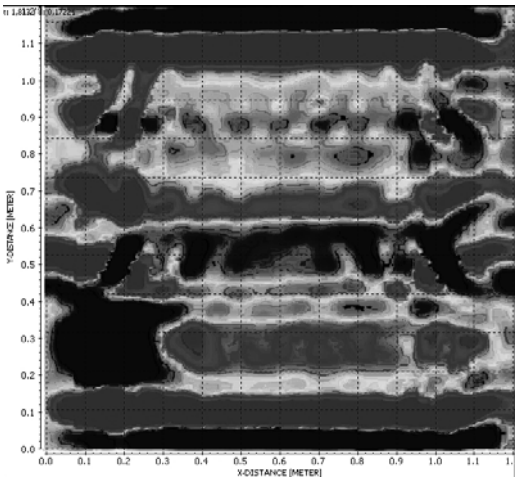

Figure 10: Image of steel plate – colour resolution (1600 MHz).

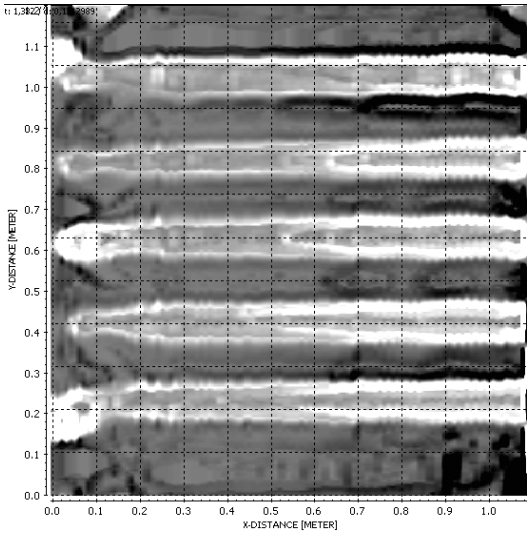

Figure 11: Image of reinforcement in the cross direction – black and white resolution (800 MHz).

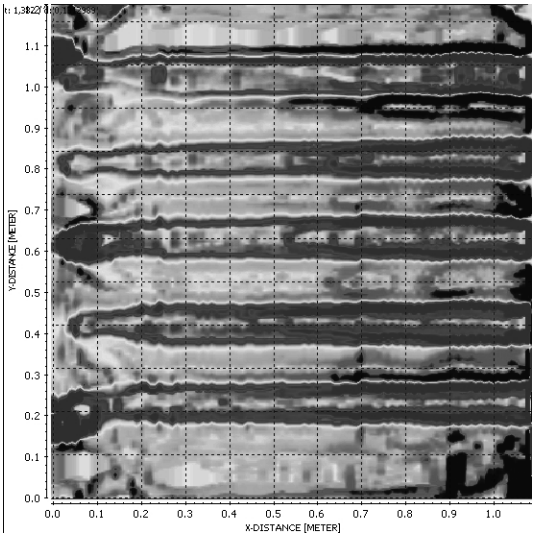

Figure 12: Image of reinforcement in the cross direction – colour resolution (800 MHz).

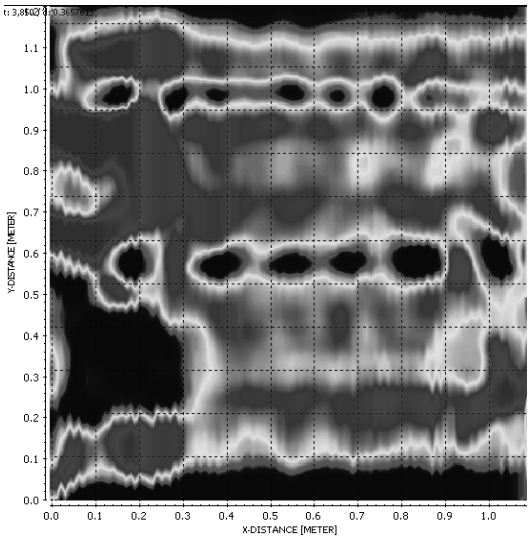

Figure 13: Image of steel plate reinforce- ment – black and white resolution(800 MHz).

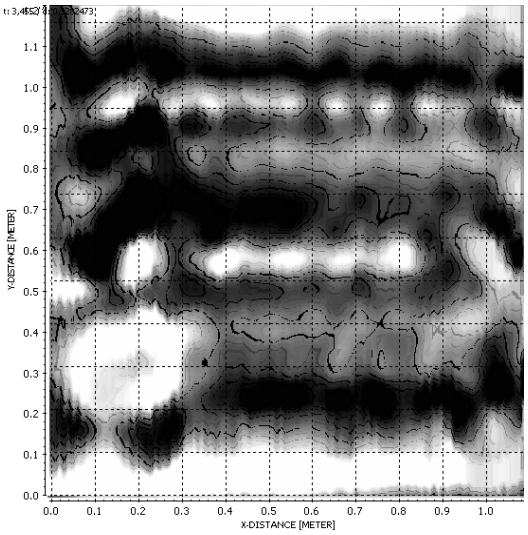

Figure 14: Image of steel plate reinfor - cement – colour resolution (800 MHz).

4.3 Evaluation of the results

On the basis of the data measured, two types of antennae were compared: 800 MHz and 1600 MHz. It was confirmed that the antenna with a transmission frequency of 1600 MHz demonstrates a considerably higher resolving power for the depth range of up to approx. 0.200 m, which is apparent from the pairs of figures: Figure 7 and Figure 11, or Figure 9 and Figure 13, and that the antenna with a transmission frequency of 800 MHz is suitable for greater depths. This measurement also confirmed that this method can be used for the detection of reinforcing elements or other anomalies in the structure.

As this was the first partial processing of a large data file, it is not possible to specify and quantify all the properties of the GPR diagnostic method. During the further processing of the data we expect specification of concrete outputs for creating a complex idea of the GPR diagnostic method.

5 CONCLUSION

The first in the series of planned experimental measurements on a physical model was focused on the comparison of applicability of two antenna systems (800 MHz and 1600 MHz) in the detection of reinforcement placed in various depths, and on monitoring the influence of the density of the measured data on the quality of the results.

The results of the measurements taken showed that the reinforcement in the given configuration was detected by both tested antenna systems, where the 1600 MHz antenna system provides, thanks to its higher sensitivity, a more detailed image of the upper parts of the examined environment, and the 800 MHz antenna system, thanks to its greater depth range, brings better results about the deeper placed non-homogeneities.

6 ACKNOWLEDGEMENTS

R&D project “Development of concrete structure diagnostics through the use of GPR scanner” has been supported and co-financed by the Czech Ministry of Industry and Trade.

REFERENCES

Chang, C. W. & Lin, C. H. & Lien, Hung S., 2009. Measurement radius of reinforcing steel bar in concrete using digital image GPR (Ground penetrating radar). Article from Construction and Building Materials.

Štainbruch, J. 2008. GPR Applicability to Thick Wall Concrete Structure Inspecion – Experiences Gained from Both Experimental Studies and Workaday Measurements. pp. 127 – 127.

The Possibilities of Nonlinear Ultrasonic Spectroscopy for the NDT in Civil Engineering

M. Manychova
Department of Building Structures, Faculty of Civil Engineering, Brno University of Technology, Brno, Czech Republic.
* *Coresponding author: manychova.m@fce.vutbr.cz*

ABSTRACT: Current methods of non-destructive ultrasonic material testing are based on the analysis of elastic wave reflection, absorption and interference. These methods are difficult to apply to inhomogeneous building materials showing tiny cracks and defects distributed throughout the specimen bulk, or in the cases where the defect size is comparable with the wavelength. Analysis of these phenomena occurring in intricate shapes is also difficult. To cope with such problems, application of wave propagation related non-linear effects and higher harmonic signal generation in the defect vicinity is advisable. Due to the presence of defects, the atomic potential energy ceases to be exactly harmonic. Second and third harmonic frequencies arise. In this domain, methods employing the non-linear acoustic spectroscopy apply. These novel defectoscopic methods are based on the non-linear behaviour of current defects and inhomogeneities regarding the elastic wave propagation processes. Unlike the electromagnetic and acoustic emission methods, which only allow the localization of currently emerging cracks and defects, the non-linear ultrasonic defectoscopy is all-defect-sensitive, thus constituting a method applicable to characterizing the quality and reliability of materials.

KEY WORDS: Nonlinear ultrasonic spectroscopic methods, inhomogeneous materials, material degradation, ceramic specimens, structural integrity

1 INTRODUCTION

Due to their assumedly higher sensitivity and more accurate quality and reliability characterization capacity, the non-linear ultrasonic spectroscopy methods are ranked among the most promising material quality and reliability characterization tools. Detailed studies of dynamic non-linearities and hysteresis in inhomogeneous media have shown that the occurrence of mesoscopic elements in the material structure gives rise to strongly non-linear dynamic phenomena accompanying the elastic wave propagation (Van Den Abeele at al. 2000, Johnson, 1999). These non-linear effects are observed in the course of the degradation process much sooner than any degradation-induced variations of linear parameters (propagation velocity, attenuation, elastic moduli, rigidity, etc.). Non-linear parameters have proved to be very sensitive to the presence of any inhomogeneities and progressing degradation of the material structure. Non-linear wave methods thus open new horizons to the acoustic non-destructive testing: they provide higher sensitivities, application speed and easy interpretation.

One of the fields in which a wide application range of non-linear acoustic spectroscopy methods may be expected is civil engineering. Poor material homogeneity and, in some cases, the shape complexity of some units used in the building industry, are heavily restricting the applicability of "classical" ultrasonic methods (Macecek, 2004). Some of the non-linear acoustic defectoscopy methods are less susceptible to the aforementioned restrictions and one may expect them to contribute to a great deal to further improving the defectoscopy and material testing methods in civil engineering.

2 NONLINEAR ULTRASONIC SPECTROSCOPY

Non-resonance methods are used to study suppressed resonance specimens. These methods can be split into two groups:

- measurements using a single harmonic ultrasonic signal (a single frequency f_1)
- measurements using multiple harmonic ultrasonic signals (usually, two frequencies f_1, f_1.)

These methods analyse the effect of non-linearities on the acoustic signals propagating through them.

2.1 Single Harmonic Ultrasonic Signal Measurement Method

In this case, where a single exciting frequency f_1 is used (Fig. 1), the non-linearity gives rise to other harmonic signals, whose frequencies f_v obey the Fourier series formulas:

$$f_v = n f_1 \qquad | n = 0, 1, 2,\ldots\infty \tag{1}$$

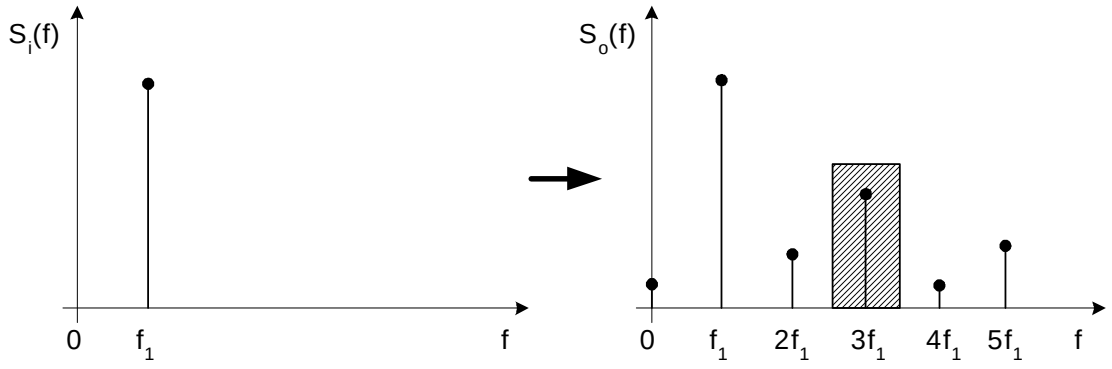

Figure 1: Frequency spectrum of a non-linear medium response.

In general, these frequency component amplitudes are falling when the harmonic order natural number, *n*, is increasing. If the non-linearity effect is not entirely symmetrical, a low-amplitude second or higher even-numbered harmonic components can arise,

whose amplitudes may be much lower than those of the odd-numbered ones. Among these emerging components, the third harmonic is the most distinctive one. Therefore, its amplitude is the one which is most frequently evaluated (Hajek & Sikula., 2005).

3 EXPERIMENT

Based on the results of our studies of building material non-linear behaviour, a measuring apparatus for diagnosing the structure integrity has been assembled.

3.1 Experimental Arrangement

A single harmonic ultrasonic signal method was applied. The measuring apparatus consisted of two principal parts, namely, a transmitting unit and a receiving unit.

The transmitting units consist of three functional blocks: a controlled-output-level harmonic signal generator, a low-distortion 100 W power amplifier and a low-pass output filter designed to suppress higher harmonic components and ensure high purity of the exciting harmonic signal.

The main chain of the receiving unit includes an input amplifier with filters designed to minimize the receiving chain distortion and a band-pass filter amplifier. Having been amplified, the sensor output signal is sampled in a DL920 transient recorder, to be subsequently saved in a computer memory for evaluation, see Fig. 2.

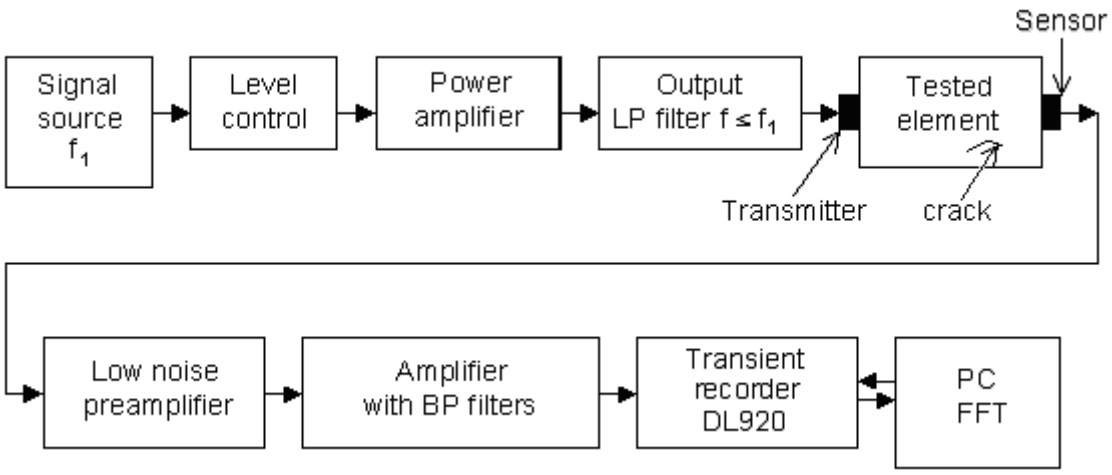

Figure 2: Block scheme of the measure equipment.

To interpret the recorded data properly, each of the measuring instruments must answer the demands of high linearity. For the purpose of improving the reliability and accuracy of the nonlinear experiments and minimizing the error effects the attention was focused to transmission between transmitter and sensors. A program package to control the measuring process, the data processing, and evaluation makes for an indispensable tool. The measurement results were represented in the form of frequency spectra.

The single-harmonic-signal non-linear ultrasonic spectroscopy method was applied to the tests of cladding elements which had been made of secondary materials. The specimens are prototypes of BIII group, fly-ash-argilic-body based ceramic cladding elements prepared

to ČSN EN 14411. Two specimen types were studied, namely, A and B. The B-type was represented by two specimens: B1 specimen, featuring an intact structure, and B2 specimen which contained a visible crack, see Fig. 3.

Two mutually perpendicular orientations of the exciter and the sensor (position 1 and position 2, see Fig. 3) were measured. An ultrasonic generator with a frequency f_1 = 29 kHz was used as a transmitter (exciter), to generate a harmonic ultrasonic wave in the specimen (Korenska & Manychova, 2008) Intact specimens were used to check whether or not the fly-ash-argilic body containing structure created the sources of signal propagation related to the non-linear phenomena. The effect of the structure defect (crack) on the propagating signal properties was studied on the B2 specimen.

The influence of exciter voltage values on transmission characteristic changes was investigated and their frequency spectra were analyzed.

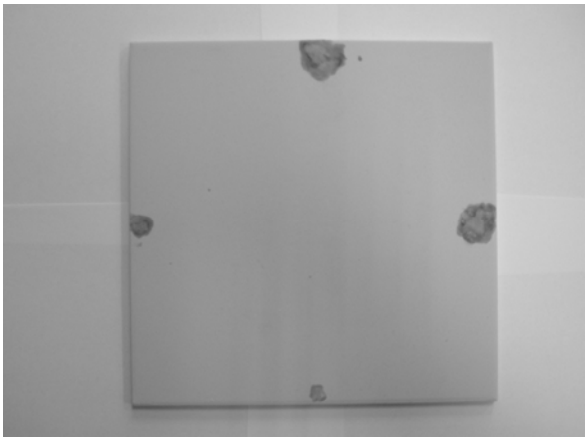

Specimen A

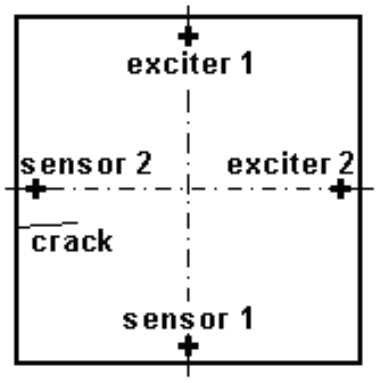

Specimen B2

Figure 3: Cladding element specimens under test.

3.2 Measurement Results

The following figures represent frequency spectra of the exciting frequency response for three different exciting voltage values. The graph in Fig. 4 represents the measurement results (position 1) of the intact sample, denoted A. From the graph a progressive decrease

of amplitudes is apparent for all voltage values. An analogous result, apart from nonlinear effects, was attained in position 2 as well.

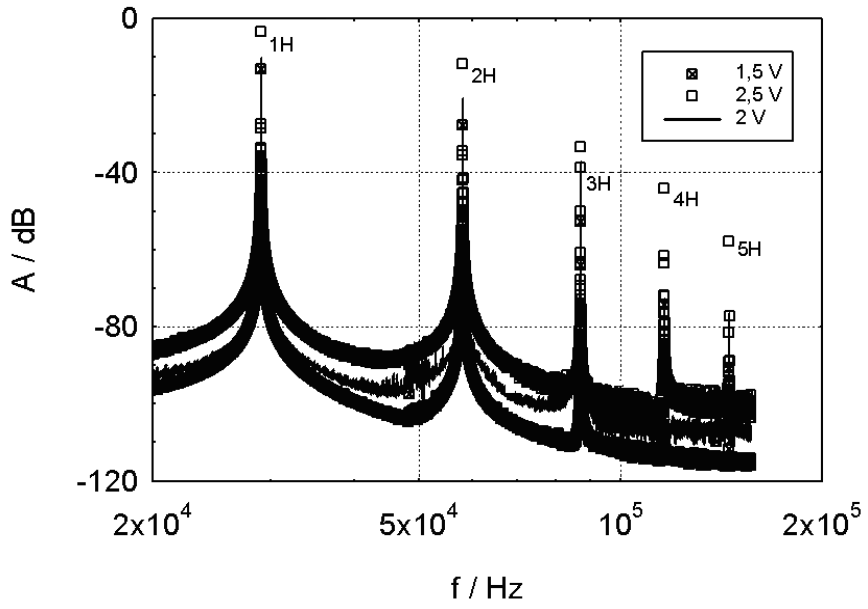

Figure 4: Frequency spectra of intact specimen A, orientation 1.

The next graph in Fig. 5 represents the measurement result of the intact sample, denoted B1. In this case analogous results, without the nonlinear effect, were reached for both positions of exciter and sensor.

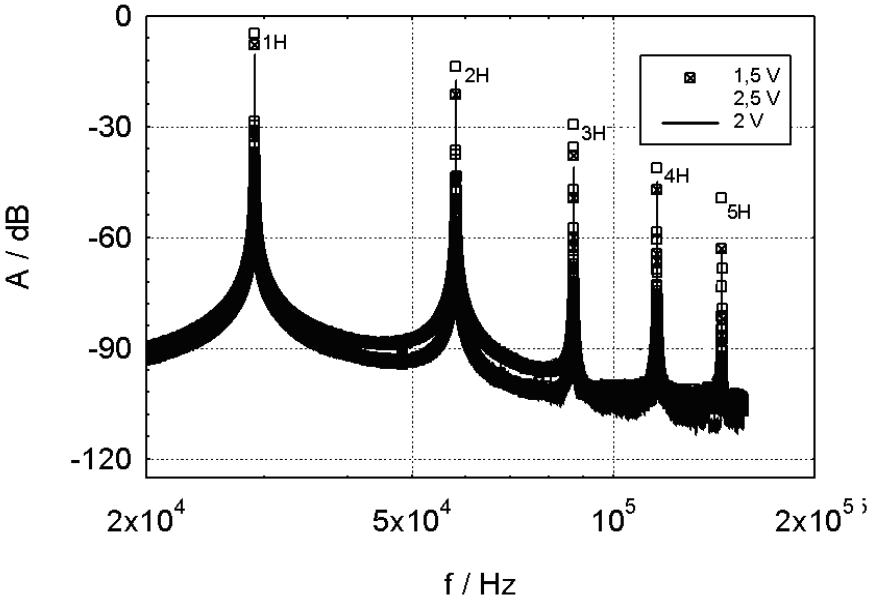

Figure 5: Frequency spectra of intact specimen B1, orientation 1.

Figs. 6 and 7 correspond to the B2 specimen with a visible crack. The graph in Fig. 5 represents the position 1 measurement result. The third harmonic component dominates in the frequency spectrum and the amplitude of the fifth harmonic is higher in comparison with the fourth harmonic component for all exciter voltage values.

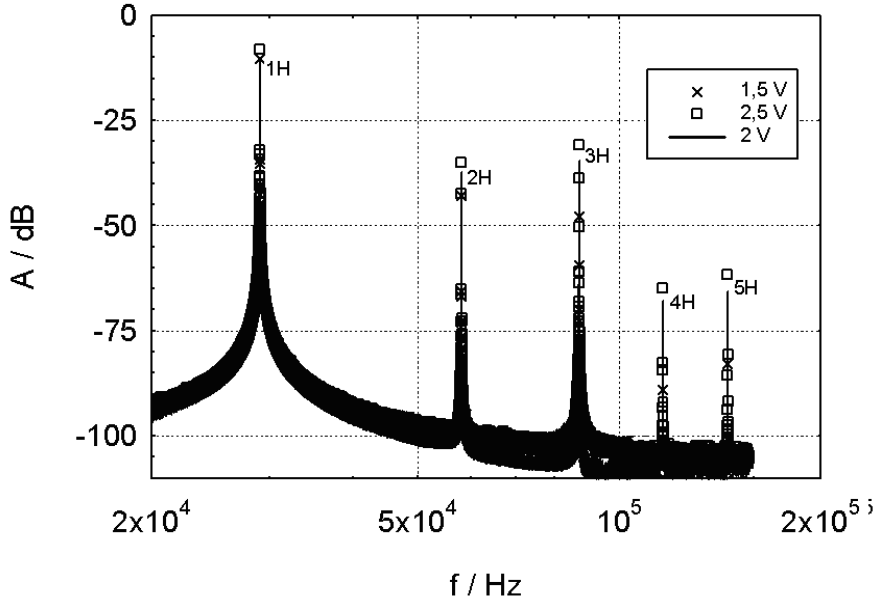

Figure 6: Frequency spectra of damage specimen B2, orientation 1.

The last graph, Fig. 7, shows the measurement result of the same specimen B2 for orientation 2; sensor was placed near the crack. In this case the second harmonic component dominates for all voltage values. The amplitudes of the fourth and fifth reach almost the same values.

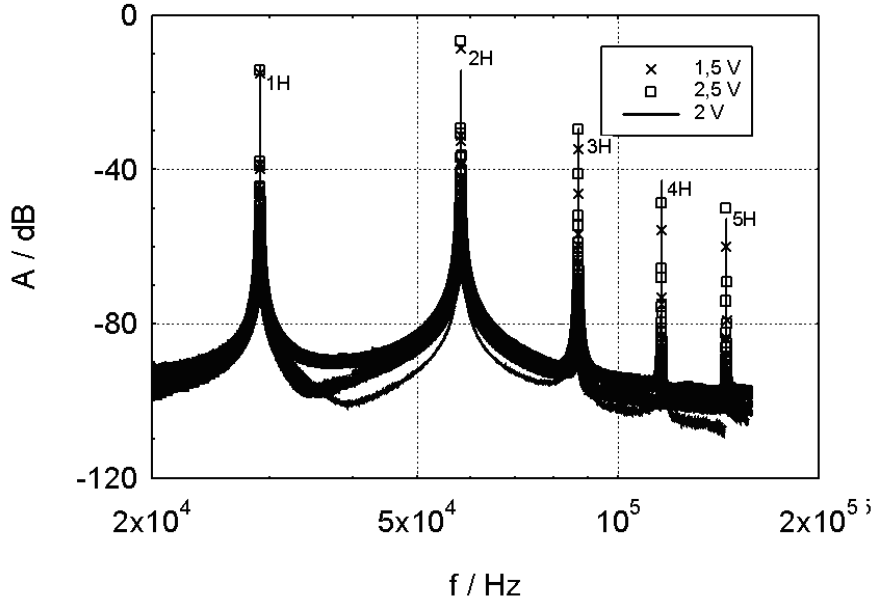

Figure 7: Frequency spectra of damage specimen B2, orientation 2.

4 CONCLUSION

The single-harmonic ultrasonic signal method was applied to advanced building materials made with the use of secondary materials. Prototypes of BIII group, fly-ash-argilic-body based ceramic cladding elements prepared to ČSN EN 14411, were tested.

Non-linear effects were analyzed for both an intact specimen and a specimen containing a defect (a crack).

a) Intact specimens were used to check whether or not the specimen inhomogeneous structure creates the source of signal propagation related non-linear phenomena. Our measurements have furnished evidence that the effect of a material's inhomogeneity is very low in the case of non-linear ultrasonic spectroscopy, its non-linear effect being substantially lower than that of common defects. The transfer function of these specimens does not feature any non-linear phenomena. The higher harmonic component amplitudes fell down progressively with an increase in the serial number *n*. Two mutually perpendicular exciter-to-sensor orientation based measurements gave identical results.

b) In the apparent crack specimen case, we focused on the transfer function variations. The transfer functions as obtained from both exciter-to-sensor configurations showed a non-linearity, which was due to the specimen structure defect. The transfer function curves differed from one another depending on the sensor-to-crack position. If the sensor was farther away from the crack, the odd-numbered (3rd and 5th) harmonic frequency amplitudes were below those of the foregoing even-numbered (2nd, 4th) harmonic components, respectively. If the sensor was fitted near the crack, an anomaly was observed, namely, the second harmonic amplitude exceeded that of the first (exciting) frequency amplitude. The fourth and fifth harmonic amplitudes reached comparable values.

ACKNOWLEDGEMENTS

This research was supported by the research project MSM 0021630511.

REFERENCES

Van Den Abeele, K. E.-A., P. A. Johnson, and A. Sutin, 2000. *Nonlinear Elastic Wave Spectroscopy (NEWS) techniques to discern material damage. Part I: Nonlinear Wave Modulation Spectroscopy (NWMS),* Research on NonDestructive Evaluation 12, pp. 17-30.

Van Den Abeele, Jan Carmeliet, James A. Ten Cate, Paul A. Johnson, 2000. *Nonlinear Elastic Wave Spectroscopy (NEWS) Techniques to Discern Material Damage. Part II: Single Mode Nonlinear Resonance Acoustic Spectroscopy.* Research on NonDestructive Evaluation 12, pp. 31- 42.

Hajek, K., Sikula, J., 2005. *Testing of Low-Current Contacts Quality and Reliability by Using Third Harmonic Distortion.* IEEE Trans. on Components and Packaging Technologies 28, pp.717 – 720.

Johnson, P. A., 1999. *The new wave in acoustic testing.* The J. Inst. Materials 7, pp. 544-546.

Korenska, M, Manychova, M., 2008. *Nonlinear Ultrasonic Spectroscopy Used to Detection of Ceramic Structure Damage.* Nonlinear Acoustics- Fundamentals and Applications,

ISNA18, pp. 541-544, Ed. Bengt O. Enflo, Claes M. Hedberg, Leif Kari, American Institute of Physics, New York 2008.

Korenska, M, Pazdera, L., Ritickova, L., 2001. *Resonant inspection – Interesting non-destructive testing tools for determine quality of tested specimen.* 6th International Conference of the Slovenian-Society-for-Non-Destructive-Testing, pp. 45-48, Ed. Grum j., Lovšin N., Slovenian Society for NDT.

Korenska, M., Chobola, Z., Sokolar, R., Mikulkova, P., Martinek, J., 2006. *Frequency Inspection as an Assessment Tool for the Frost Resistance of Fired Roof Tiles.* Ceramics-Silikáty, vol. 50, iss. 3, pp. 185 – 192.(2006).

Macecek, M., 2003. *Ultrasonic Concrete Testing.* 33rd International Conference Defektoskopie 2003, pp. 117-132, Ed. Mazal P.

NDT of Mechanical Damaged Concrete Specimens by Nonlinear Acoustic Spectroscopy Method

M. Matysik* & I. Plskova & M. Korenska
Department of Physics, Faculty of Civil Engineering, Brno University of Technology, Veveri 331/95, 602 00 Brno, Czech Republic
** Corresponding author: matysik.m@fce.vutbr.cz*

B. Kucharczykova
Institute of Building Testing, Faculty of Civil Engineering, Brno University of Technology, Veveri 331/95, 602 00 Brno, Czech Republic

ABSTRACT: Current research and development of non-linear ultrasonic spectroscopy methods shows these methods to be very promising for material testing and defectoscopy in the near future. Our experiments focused on the testing of lightweight concrete specimens using the single-frequency excitation method. We studied the concrete specimens' structure after having been stressed by a mechanical force. Measurements were realized before and after mechanical loading.

KEY WORDS: non-linear acoustic spectroscopy, light concrete, freeze-thaw cycles

1 INTRODUCTION

According to the relevant standards, there are three kinds of concrete: lightweight, plain and heavyweight concrete. By definition, the volume mass of lightweight concrete is less than 2000 kg/m^3. Depending on the intended application, the lightweight concrete group consists of three subgroups: thermal insulating lightweight concretes, their intended application falling into the thermal insulation field, furthermore, structural insulating lightweight concretes, their function being both supporting and insulating, and, last but not least, structural lightweight concretes, whose main function is their bearing capacity and the main requirement is strength combined with low volume mass. (Kucharczykova & Kersner, 2008; Korenska et al. 2005, Plskova et al. 2009)

On the basis of non-linear effect studies, new NDT methods have been designed (Van den Abeele et al. 2000, Zaitsev et al. 2006). These methods are based on the elastic wave non-linear spectroscopy. Existing linear acoustic methods focus on the energy of waves reflected at structural defects, analyzing the reflected wave energy, wave velocity or amplitude variations. However, none of these "linear" wave characteristics is as sensitive to small cracks as the specimen non-linear response (Nagy, 1998; Van den Abeele et al. 2001; Van den Abeele et al. 2009). In this way, non-linear methods thus open new horizons in non-destructive acoustic testing, providing undreamed-of sensitivities, application speeds and easy interpretation. One of the fields in which a wide application range of non-linear acoustic spectroscopy methods can be expected is civil engineering, for example, for fatigue damage assessment (Nagy, 1998), micro-damage diagnostics (Van den Abeele et al. 2001; Chen

2008), or monitoring of the early hydration process in concrete (Van den Abeele et al. 2009). It is predicted that these advanced techniques can contribute a great deal to the improvement and refinement of the NDT methods in the building industry practice.

2 EXPERIMENT

Lightweight concrete specimens have been studied in our experiments. A fresh concrete mix consisted of the following: 0-4 mm natural gravel and sand, Liapor CZ4-8/600 lightweight porous aggregates, CEM I – 42,5 R cement, fly-ash, plasticiser and water. Water and lightweight porous aggregates were gauged by volume; all other components were gauged by mass.

Joists of dimensions 100 × 100 × 400 mm were made of the lightweight concrete. To produce the test specimens, moulds were filled progressively in two layers, each of them being vibrated for a period of 30 seconds. After 24 hours, the joists were removed from the moulds to be placed into a tank with PE foil covered wooden slat grids and a constant water level at the bottom. The tank was kept in the laboratory at a temperature of 20 ± 1°C and relative humidity RH 50 ± 5 %. The joist volume mass amounted to 1700 kg/m^3 after 28 days.

Hardened concrete specimens were prepared for pressing machine tests. A notch 8 mm wide and 33 mm deep (one third of the joist height) was cut at the joist centre – see Fig. 1. Subsequently, first specimen measurements were carried out prior to the pressing machine tests.

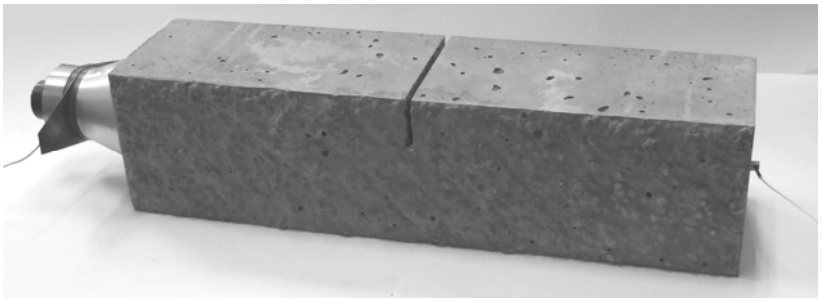

Figure 1: Joist fitted with exciter and sensor.

In the pressing machine, the joist was placed on 2 supports. Force F was applied to the joist at its centre (see Fig 2) – which is the case of three-point bending of a notched joist. The force F was increased gradually until a crack occurred (it arose at the notch root, Fig. 3). The force grew very slowly in order to prevent joist breakage, only the formation of a crack being desirable. Subsequently, the second specimen measurement stage was carried out.

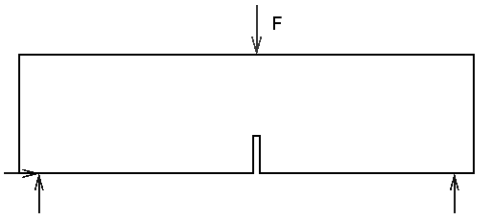

Figure 2: Three-point bending of a notched joist.

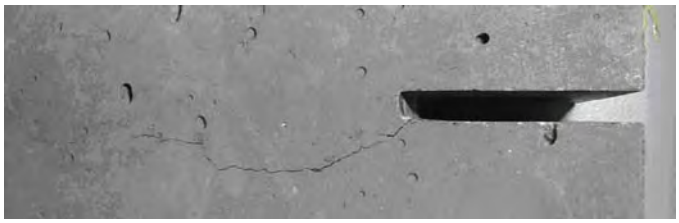

Figure 3: Post-stress LC_09_01 specimen – detailed view of the crack.

3 MEASURING METHOD

We classify non-linear acoustic spectroscopy methods into resonant and non-resonant (Korenska & Manychova, 2008; Hajek & Sikula, 2008). Non-resonance methods are used to study suppressed resonance specimens. These methods analyze the effect of nonlinearities on acoustic signals propagating through them. These methods can again be split into two groups (Korenska & Manychova, 2008): measurements using a single harmonic ultrasonic signal (single exciting frequency) and measurements using multiple harmonic ultrasonic signals - mostly two exciting frequencies. There is also the possibility to combine one ultrasonic and one electrical signal with different frequencies (Sikula et al. 2008).

We pay particular attention to the single harmonic ultrasonic signal measurement method which was used in the experimental part.

4 MEASURING APPARATUS

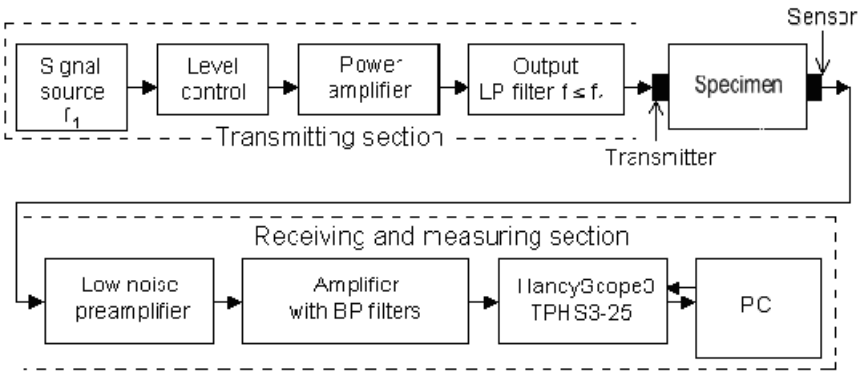

Figure 4: Block diagram of the measuring apparatus.

The transmitting section of measuring apparatus consists of four functional blocks: a controlled-output-level harmonic signal generator, a low-distortion 100 W power amplifier, an output low-pass filter to suppress higher harmonic components and ensure the high purity of the exciting harmonic signal and a piezoceramic transmitter (actuator) to ensure the ultrasonic excitation.

The receiving section consists of a piezoceramics sensor, a low noise preamplifier with classical or differential input connector, an amplifier with band - pass filters and a spectral analyzer. In our case the spectral analyzer was the oscilloscope HandyScope3 TPHS3-25 controlled by computer.

For the recorded data to be interpreted properly, each of the measuring instruments must meet the following criteria:

- High linearity of all instruments (generators, amplifiers, sensor, transmitter,…).
- High resolution in the frequency domain.
- High dynamic range (90 to 130 dB).
- Highly efficient filtration of detected signals (fundamental frequency suppression).
- Frequency range 10 kHz to 10 MHz.
- Optimized sensor and transmitter location.

A program package to control the measuring process and the data processing and evaluation makes an indispensable tool.

5 MEASUREMENT RESULTS

The measurement results are presented in figures 5 and 6. They show the frequency spectra from both measurement stages, prior to and after the pressing machine test.
In Fig. 5, a change in the specimen response is seen to correlate with the specimen structure change. The pre-stress curve features an amplitude fall with growing harmonic frequency order, no non-linearity being apparent. The post-stress frequency spectrum, corresponding to the specimen structural integrity being impaired, shows – in consequence of higher damping – lower amplitudes by about 20 dB. The fourth and the fifth harmonic components vanished almost entirely. Several other frequency components are emphasized in the spectrum.

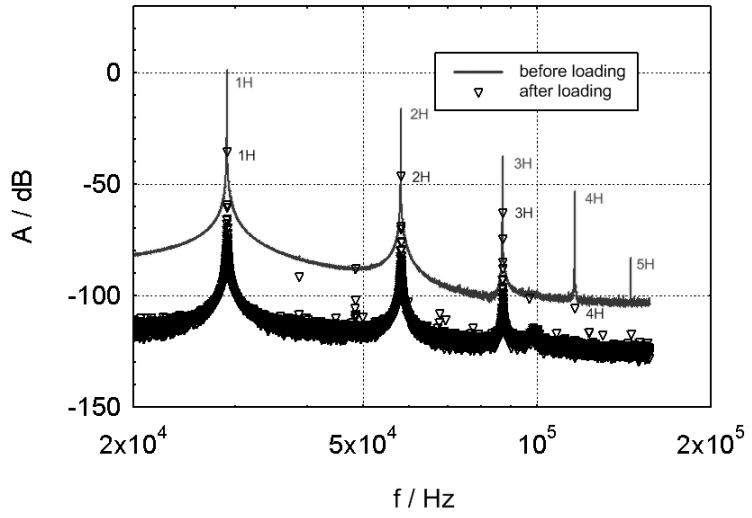

Figure 5: Frequency spectrum – specimen LC_09_01.

In the frequency spectrum of post-stress LC_09_02 specimen measurement, Fig. 6, a change in the second harmonic frequency is seen. Its amplitude is comparable with that of the first (exciting) harmonic. The fourth and the fifth harmonic frequency components almost vanished again. Several components of various frequencies are observed in the spectrum. Other specimens provided similar results.

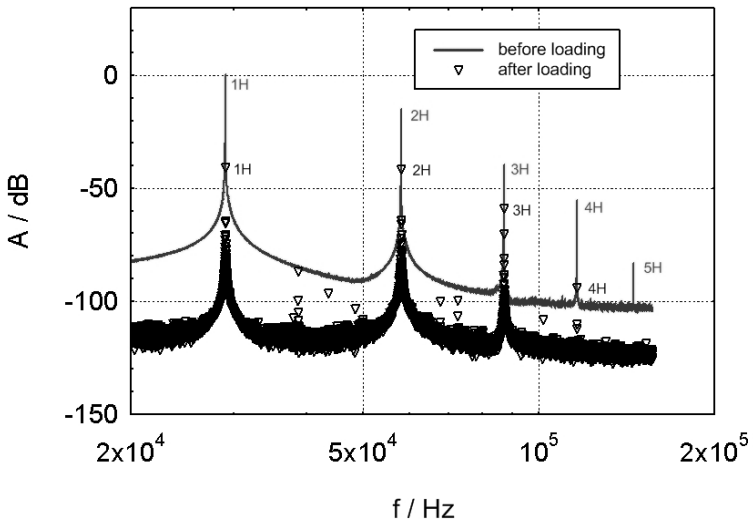

Figure 6: Frequency spectrum – specimen LC_09_02.

6 CONCLUSION

The following pieces of knowledge follow from the result analysis:

- High inhomogeneity induced non-linear effects are substantially weaker than those due to “normal” defects.
- The notch forced into the joist does not make a source of non-linear phenomena.
- Material structure defects give rise to non-linear effects during the signal transmission.

7 ACKNOWLEDGEMENT

This research is supported by Czech Science Foundation - project GP103/09/P252 and by Ministry of Education, Youth and Sports, project No. 1M06005, within the activities of the CIVAK research centre.

REFERENCES

Kucharzcyková, B., Keršner, Z. 2008. *Fracture properties of lightweight concrete: Influence of specimen age*. In Proceedings of the International Conference LC2008, Brno, Akademické nakladatelství CERM, 2008, p. 174 – 179.

Van Den Abeele, K.E.-., Johnson, P.A. and Sutin, A., 2000. Nonlinear Elastic Wave Spectroscopy (NEWS) techniques to discern material damage, Part I: nonlinear wave modulation spectroscopy (NWMS). *Research in Nondestructive Evaluation,* 12(1), pp. 17-30. ISSN: 09349847

Van Den Abeele, K.E.-., Carmeliet, J., Ten Cate, J.A. and Johnson, P.A., 2000. Nonlinear elastic wave spectroscopy (NEWS) techniques to discern material damage, Part II: single-mode nonlinear resonance acoustic spectroscopy. *Research in Nondestructive Evaluation,* 12(1), pp. 31-42. ISSN: 09349847

Zaitsev, V., Nazarov, V., Gusev, V. and Castagnede, B., 2006. Novel nonlinear-modulation acoustic technique for crack detection. *NDT and E International,* 39(3), pp. 184-194. ISSN: 09638695

Nagy, P.B., 1998. Fatigue damage assessment by nonlinear ultrasonic materials characterization. *Ultrasonics,* 36(1-5), pp. 375-381. ISSN: 0041624X

Van Den Abeele, K.E.-., Sutin, A., Carmeliet, J. and Johnson, P.A., 2001. Micro-damage diagnostics using nonlinear elastic wave spectroscopy (NEWS). *NDT and E International,* 34(4), pp. 239-248. ISSN: 09638695

Chen, X.J., Kim, J.-., Kurtis, K.E., Qu, J., Shen, C.W. and Jacobs, L.J., 2008. Characterization of progressive microcracking in Portland cement mortar using nonlinear ultrasonics. *NDT and E International,* 41(2), pp. 112-118. ISSN: 09638695

Van Den Abeele, K., Desadeleer, W., De Schutter, G. and Wevers, M., Active and passive monitoring of the early hydration process in concrete using linear and nonlinear acoustics. *Cement and Concrete Research,* . in print ISSN: 00088846

Stauffer, J.D., Woodward, C.B. and White, K.R., 2005. Nonlinear ultrasonic testing with resonant and pulse velocity parameters for early damage in concrete. *ACI Materials Journal,* 102(2), pp. 118-121. ISSN: 0889325X

Korenska, M. and Manychova, M., 2008. Nonlinear ultrasonic spectroscopy used to detection of ceramic structure damage. *Nonlinear Acoustics Fundamentals and Applications, Aip Conference Proceedings.* 18th International Symposium on Nonlinear Acoustics, Stockholm, Sweden, 2008, pp. 541-544. ISSN: 0094243X, ISBN: 9780735405448

Sikula, J., Sedlakova, V., Navarova, H., Tofel, P., Majzner, J. and Hajek, K., 2008. NDT of conducting solids by electro-ultrasonic spectroscopy, 2008, *Nonlinear Acoustics Fundamentals and Applications, Aip Conference Proceedings.* 18th International Symposium on Nonlinear Acoustics, Stockholm, Sweden, 2008, pp. 319-322. ISSN: 0094243X, ISBN: 9780735405448

Hajek, K. and Sikula, J., 2008. A resonance frequency shift in spectral analysis of the impact echo. *Nonlinear Acoustics Fundamentals and Applications, Aip Conference Proceedings.* 18th International Symposium on Nonlinear Acoustics, Stockholm, Sweden, 2008, pp. 525-528. ISSN: 0094243X, ISBN: 9780735405448

Korenska, M., Pazdera, L., Pospisil, K., Stryk, J. and Vyroubal, P., 2005. Detection of the reinforcement corrosion in prestressed concrete girders. *Application of Contemporary Non-Destructive Testing in Engineering.* 8th International Conference of the Slovenian-Society-for-Non-Destructive-Testing on the Application of Contemporary Non-Destructive Testing in Engineering. Portoroz, Slovenia, 2005. pp. 317-322. ISBN: 9619061055

Plskova, I.; Kucharczykova, B.; Matysik, M.; Chobola, Z. 2009.*Non-Destructive Testing of Lightweight Concrete Specimen by Impact-Echo Method*. The e-Journal of Nondestructive Testing, 2009, 14(3), p. 1 - 6.

Mazal, P.; Pazdera, L., 2005. *Advanced Acoustic Emission Signal treatment in the Area of Mechanical Loading*. In The *8th Int.Conf. of the Slovenian Soc.for NDT "Application of Contemporary NDT in Engineering"*. Portorož, SSNDT Slovenia. 2005. pp. 283 - 292. ISBN 961-90610-5-5.

Korenska, M.; Pazdera, L.; Pospisil, K., 2006. Detection of the reinforcement corrosion in pre-stressed concrete girders. *International Journal of Microstructure and Materials Properties* . 2006. 2006(1)(3/4). p. 374 - 382. ISSN 1741-8410.

Use of Palmtop Computers for Monitoring Traffic

M. Bíl* & M. Bílová & J. Martínek
Transport Research Centre, Czech Republic.
**Corresponding author: michal.bil@cdv.cz*

ABSTRACT: On the basis of a cycling traffic count carried out in the town of Olomouc a new method of monitoring traffic was presented based on the use of palmtop computers (PDAs). For short-term traffic counts, this method may entirely replace the commonly used paper forms. In addition, this method provides more possibilities, namely the recording of the exact time of vehicle passing and a description of the direction of vehicle movement. Almost all the software used for the preparation and processing of data is freely available, which allows all interested people to use this method.

KEY WORDS: Monitoring, traffic count, palmtop computer, PDA, cycle traffic.

1 INTRODUCTION

For responsible decision-making in planning the construction of new roads it is necessary to have an idea of their future traffic loads. This applies both to roads used for motor traffic and to the network of cycle paths and cycle routes. Applications for grants for the construction of cycle paths require data on the numbers of vehicles that use a given road. Likewise, it is good to know the number and demographic structure of cyclists who frequent these roads. To meet these requirements manual monitoring of cycling traffic is usually carried out. The data thus obtained can also be used to study the use of bicycles.

Cycling can be performed for the following purposes:

Commuting – regular or occasional commuting to work, school, etc. Since 2001, this kind of bicycle use has been monitored by, for example, a questionnaire survey carried out by the Czech Statistical Office. This is also the principal argument for the sake of the construction of cycle paths. Their separation from motor traffic should improve road traffic safety (KONKIN et al., 2006; RICHTER et al, 2007).

Recreation – concerns occasional rides, usually on terrain which is different from that used when commuting rides are taken. Surveys of recreational cycling are carried out especially in major tourist areas, where it belongs to the category of "monitoring of visitors" (e.g., COPE et al., 2000). The initiative of the National Park České Švýcarsko, where, since 2008, the frequency of cycling has been monitored with the use of automatic sensors, is an example of cycling traffic counts in Czech natural areas (verbal information). But cycle tourists also like to use the backbone network of cycle routes of the systems EuroVelo and North Sea Cycle Route, (e.g. LUMSDON et al, 2004.).

Sport or training – the terrain, type of a bicycle and ride intensity differ according to the kind of sport practiced.

The monitoring of cycling should always be organized in a way which allows for distinguishing between all kinds of bicycle use. For example, it is desirable to monitor commuting to work before the anticipated beginning of working hours, i.e., in the morning. In the afternoons there is already a likelihood of data "contamination" by recreational cycling traffic.

According to the objectives and the method used it is possible to divide traffic monitoring generally into the two following categories:

1. the collection of quantitative data, particularly on the frequency of a given vehicle type, which is usually called the traffic count,
2. the collection of socioeconomic and demographic parameters of drivers and passengers, which is usually performed in the form of questionnaire surveys or interviews.

A traffic count is either carried out manually or with the use of automatic, mostly electronic, counters. These counters are useful if it is necessary to count for a relatively long period, e.g., one week and longer. There are many technologies that can be used for the detection of cyclists (pressure sensors, infrared detectors, induction loops, etc.). But the use of most available methods is considerably limited in that they can not be used to determine some other characteristics of cyclists, such as the age, sex, clothing, helmet, etc. Limitations of most sensors include the fact that they can not distinguish a cyclist from a pedestrian, or a cyclist from a car. Though it is possible to connect a movement sensor with a camera and make an image analysis, the obtained results – unlike those for the detection of motor vehicles – have so far been unsatisfactory for the monitoring of cycling. There have been promising attempts to distinguish cyclists and motorcyclists (MESSELODI et al., 2007), however similarly to the video detection of cyclists and pedestrians (HEIKKILA and SILVÉN, 2004), they do not yet have commercial applications.

For occasional campaign counts where it is required to find out the current traffic situation at several places, a counting staff is employed. They enter data, usually sums for a given type of vehicle, into pre-prepared paper forms. Regular traffic counts organized by the Road and Motorway Directorate of the Czech Republic (RSD) are carried out this way. Shortcomings of this process involve the necessity to subsequently retype the data into a PC, and the potential errors introduced thereby. Another limitation consists of the inability to record the exact time of passing of a given vehicle. The sums relate to the day of counting.

The process of data collection that we present fills the gap between the automatic data collection (traffic count) on the one hand, and the questionnaire survey on the other hand. It has a potential to streamline the work of the counting staff by introducing electronic forms in a PDA environment, and an intuitive pseudo-map interface directly on the device display.

2 METHODS

To entirely replace paper forms and enhance the monitoring by introducing other potentialities that involve, in particular, recording the exact time of a vehicle passing, we therefore used palmtops - PDAs (Personal Digital Assistant). The advantages of PDAs when compared to paper forms consist particularly of the following:

a. Once downloaded to a PC the data collected is immediately available, so there is no need to retype it, which is often a source of errors.
b. Nowadays, PDA technology is easily accessible. It is not financially demanding and can be used for everyday work as an organizer, etc.
c. It is possible to adjust the appearance of counting forms for a particular event and the environment to match the situation at a particular place (unlike Traffic Data Collectors, which represent mobile devices designed as a hardware module for traffic counts at intersections – e.g., the Jamar technology).
d. A great advantage of PDAs lies in the possibility to record the time of a vehicle passing, making these data applicable for further use. This constitutes an important connection between the conventional counting and filling in forms.

For traffic counts only such a device can be used that can operate in a battery mode for the time needed to collect data, which is usually several hours. If ***there's*** bad weather it is good to have the possibility to use a rain protective cover.

The preparation of the form for work is as follows. The PC needs to have XS Designer software installed, which is the environment for the form production. A single form may contain more pages, which may include different controls such as: descriptions, text boxes, check boxes, option buttons, combo boxes, date and time, pictures and buttons. An action can be set for each control, either by selecting from predefined controls, or by creating customized ones in the programming languages JScript or VBScript. In addition, SQL inquiries can be defined and assigned to controls of the form. Operation of the form can be tested under condition that XSForms software is installed on PDA and the PDA is connected to a computer.

We had 10 pieces of PDA, type Fujitsu SIEMENS FSC Pocket LOOX N560 with an active touch screen at our disposal. During the preparatory phase we prepared plans of given counting sites in the programme PhotoFiltre. These sites were usually located at intersections, where each of the four directions was assigned a letter A – D (Figure 1). The software PhotoFiltre is a simple graphic editor for creating and editing raster images. Among other things, it also supports working with layers. To create and transfer the prepared form from PC to PDA, we used the programme XSDesigner. In PDA, the form can be opened in the programme XSForms which cooperates with XSDesigner.

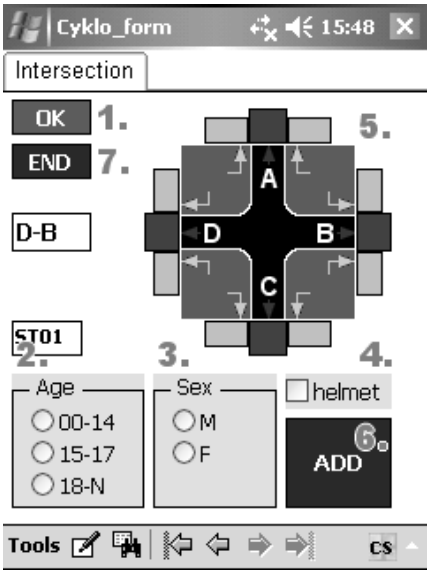

Figure 1: Example of a form in PDA.

Prior to each measurement, the counting staff met together to synchronize the time in their PDAs with an accuracy in seconds. Then everyone went to their stands and at a given time, in our case at 5:30, started the traffic count by pressing the ”Start“ button on his/her PDA display (see Figure 1).

The passing of the first cyclists through the intersection was then awaited. Given that the counting sites had been chosen to provide the staff with a good view, it was possible to estimate the cyclist's age, sex, and the presence of a protective helmet prior to his/her approach to a counting site. Once the direction had been evident in which the cyclist would leave the intersection, his/her passage route was recorded (point 5 in Figure 1). When passing straight through the intersection, the middle of the three buttons (red) was pressed for the direction in which the cyclist had left the intersection. If he/she had ridden, for example, from D to B, the middle button was pressed for B. If the cyclist had turned, the outer buttons (yellow) were pressed. For example, if he/she had turned from D to A, the left button was pressed for A. This intuitive interface with active elements on the display makes the work very quick.

By pressing the “Add” button the exact time of cyclist's passing was entered. At the end of the count at 8:00 am the “End” button was pressed to finish the data collection and close the programme. If, within the counting process, the staff had become aware of some errors made, it was still possible to correct them at the count site. The form allows moving between records (arrows in the lower part of the form).

In the course of the count the staff were in connection with the coordinator of the action via mobile phones. It was therefore possible to operatively aid the staff if the count was jeopardized by a drop of battery voltage on some particular PDA. To solve such situations, the traffic count coordinator was equipped with a mobile power pack - APC Mobile Power Pack UPB10.

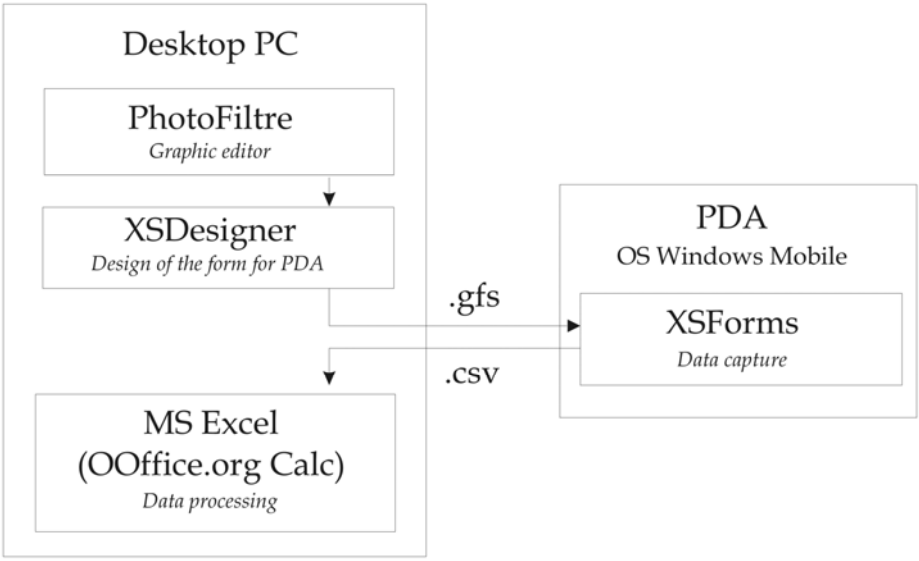

Figure 2: Diagram of the procedure of data preparation and processing.

After finishing the traffic count the form was directly exported in the application XSForms to a new file in CSV format. This file was subsequently transferred to a desktop computer using the software Microsoft ActiveSync which is used for synchronizing mobile devices with the system Windows Mobile. Using a PC data were imported into the programme MS Excel for analysis of the volumes of cyclists riding in individual directions and at certain times. This procedure is schematically illustrated in Figure 2.

Although the whole working process is very efficient, it is necessary to reckon with some constraints, especially for older hardware. These constraints may particularly involve the worse screen readability of PDAs outdoors, lower battery life (usually less than 3 hours depending on the intensity of the display backlight), and the capability of PDAs to work at lower temperatures.

Regarding the work coordination it is necessary to not forget to synchronize the time before the start of a count.

3 APPLICATION

We initially applied this method to carry out a cycling traffic count in the town of Olomouc. Due to the fact that the centre of the town is a historical reserve with the original historic pavement, it is not convenient for this type of transport. In its vicinity, however, there is an almost perfectly coherent system of urban parks which follow the foreground of a former fortress. Also the topography of the town favours the use of bicycles.

The network of cycle paths in Olomouc has been built and expanded since 1994. The total length of available cycle paths within the territory of the town is 23 km, but cyclists also frequently use the network of streets that they share with motor vehicles (TÁZLAR, 2007). We focused our research only on the vicinity of the centre where we identified 10 counting sites. We placed an emphasis on detecting the main routes for commuting to work.

The cycling traffic count was carried out in March 2009 within two weeks (10 – 12 March, and 17 – 19 March) on Tuesdays to Thursdays from 5:30 am to 8:00 am in order to cover the middle of a working week (we assume that on Mondays and Fridays, commutation may have a different pattern), and morning commutes to work and schools. The cycling traffic count was carried out off the main cycling season because we focused mainly on those cyclists who commute regularly. In our opinion the seasonal cyclists would not commute during this time, as well as those cyclists for whom cycling is a leisure activity. We prepared a data sample based on an exemplary day, Wednesday, 18 March, in order to provide an introduction to the traffic count method with the use of PDA.

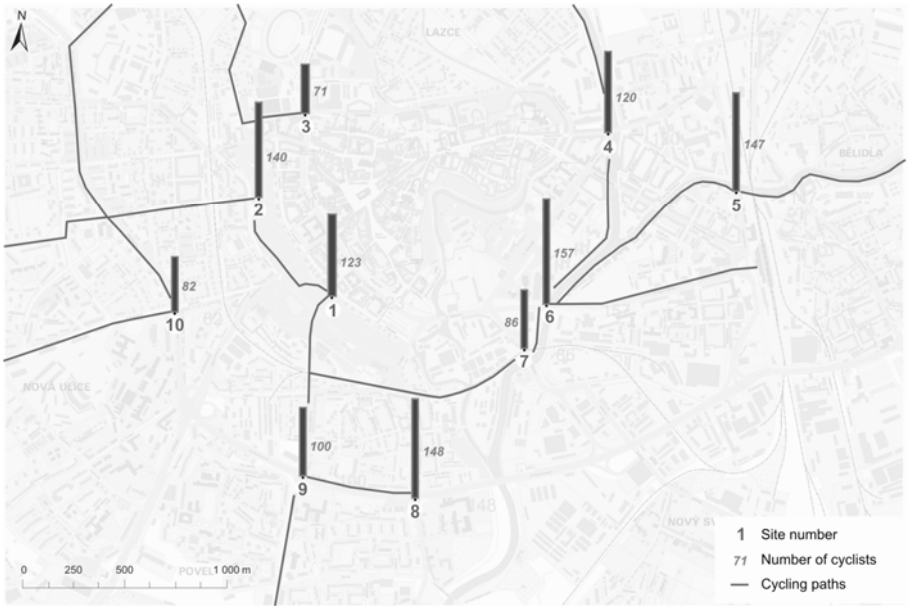

Figure 3: Number of cyclists passing traffic count sites and their localization in the selected part of the town of Olomouc.

Figure 3 shows the centre of the town of Olomouc. The dark line marks the constructed parts of cycle paths that are separated from motorised traffic. Since the network is still incomplete, the cyclists need to use roads for motorised traffic, too. The height of columns and numbers next to them show the number of cyclists who passed a traffic count site on that day between 5.30 a.m. and 8.00 a.m., regardless of the direction of riding.

Figure 4: Direction of movement of cyclists within stations 6 and 7.

Figure 4, traffic count sites of 6 and 7, shows the visualized results in GIS. The displayed digital form has the advantage of capturing the direction of movement of cyclists. Individual columns vary in colour, based on the fact whether cyclists arrive at a traffic count site (black) or depart from a traffic count site (grey).

Table 1: Recorded cyclists having passed traffic count sites 6 and 7 at times 5.30 – 6.00 on 18 March 2009.

Direction from no.	Departure (hh:mm:ss)	Arrival (hh:mm:ss)	Speed (km/h)	Sex	Helmet (Y/N)	Age group
6	5:35:20	5:36:05	20	M	Y	>18
7	5:37:15	5:37:58	21	M	N	>18
7	5:38:00	5:38:52	17	M	N	>18
6	5:42:34	5:43:13	23	F	N	>18
7	5:45:07	5:45:56	18	M	N	>18
6	5:48:41	5:49:11	30	F	N	>18
6	5:53:17	5:53:56	23	M	Y	>18
7	5:54:55	5:55:33	24	M	Y	>18
7	5:54:01	5:54:57	16	M	Y	>18
7	5:58:10	5:58:58	19	M	Y	>18

Table 1 shows the outcome of counting in the table processor application in order to determine the average speed of a cyclist. In the morning between 5.30 a.m. and 6.00 a.m. six cyclists arrived at site 6 (direction from site 7) out of the total daily number of 27 cyclists arriving from that direction, see Figure 4. Four cyclists (out of 13 arriving, or 28 departing cyclists) arrived at site 7 (direction from site 6).

4 DISCUSSION AND CONCLUSION

The method we propose can replace conventional traffic volume counts carried out with the use of paper forms. In addition, it also allows for the recording of exact times of passing of selected road users (in this case – a cyclist). Similarly to situations where a motion sensor is installed in the site of a traffic count profile, we obtain information on the volumes of cycling traffic at arbitrary time steps, but also further data, e.g., safety helmet wearing, age group, sex, reflective clothes, etc. Monitoring at intersections allows for the recording of information about travel directions.

We can only benefit from the advantages of the use of pocket PCs – PDAs compared with the use of paper forms if these devices meet the requirement of several hours' operation in the field. The whole working process and the process of data processing uses software which is either freely available or widely used and can be easily substituted (e.g., MS Excel for OpenOffice Calc).

Although there are sophisticated devices for traffic counting on junctions (e.g. Traffic Data Collector by Jamar Technologies, Inc), our introduced solution is flexible thanks to the fact that a customized form design (junction) can be prepared in advance and controls deployed according to the needs and purpose of an action.

5 ACKNOWLEDGMENT

For their cooperation in the cycling traffic count carried out many thanks to the employees and students of the Department of Geoinformatics of the Faculty of Science of the Palacký University in Olomouc. Our contribution was supported by the project of the Ministry of Transport No. MD04499457501.

REFERENCES:

Cope, A. – Doxford, D. – Probert, C. *Monitoring visitors to UK countryside resources. The approaches of land and recreation resource management organisations to visitor monitoring.* Land Use Policy, 17, (2000) 59-66.

HeikkilA, J. – Silvén, O. *A real-time system for monitoring of cyclists and pedestrians.* Image and Vision Computing 22 (2004) 563–570.

Konkin, D.E. – Garraway, N. – Hameed, S.M. – Brown, D.R. – Granger, R. – Wheeler, S. – Simons, R.K. *Population-based analysis of severe injuries from non-motorized wheeled vehicles.* The American Journal of Surgery, 191, 615–618, 2006.

Lumsdon, L. – Downward, P. – Cope, A. *Monitoring of cycle tourism on long distance trails: the North Sea Cycle Route*. Journal of Transport Geography 12 (2004) 13–22.

Messelodi, S. – Modena, C.M. – Cattoni, G. *Vision-based bicycle/motorcycle classification*. Pattern Recognition Letters 28 (2007) 1719–1726.

Richter, M. – Otte, D. – Haasper, C. – Knobloch, K. – Probst, C. – Westhoff, J. – Sommer, K. – Krettek, C. *The Current Injury Situation of Bicyclists-A Medical and Technical Crash Analysis,* J Trauma. May;62(5):1118-22, 2007.

Tázlar, J. *Mapping of cyclist infrastructure on the territory of the town of Olomouc*, 2007. 58p. Diploma thesis on the Faculty of Science of the Palacký University in Olomouc, Department of Geoinformatics. Supervisor of diploma thesis - Michal Bíl.

Ground Penetrating Radar as a Tool for the Diagnostics of Concrete Pavements

J. Stryk* & R. Matula
Department of Infrastructure and Environment, CDV – Transport Research Centre, Brno, Czech Republic
** Corresponding author: josef.stryk@cdv.cz*

ABSTRACT: This paper describes the basic possibilities for the usage of ground penetrating radar (GPR) in road diagnostics. The opportunity for multi-channel GPR use and the limitations arising from measurements performed at high speeds are described. Particular attention is paid to the problems of the diagnostics of concrete pavements. The radar configuration used for location of dowel bars and tie bars is presented.

KEY WORDS: Ground penetrating radar, GPR, diagnostics, pavement, guidelines.

1 GROUND PENETRATING RADAR

GPR is a piece of equipment which uses high frequency electromagnetic waves. In combination with suitable software it provides the location and an evaluation of the electrical and magnetic features of the studied environment in which these waves radiate.

The boom in GPR usage started with the commercial selling of this equipment by the American company GSSI in 1972. GPR started to be used in a lot of different areas of human activity. One of these areas is in the diagnostics of roads and bridges, which is a common event nowadays (Fauchard et al. 2000), (Al-Qadi et al. 2003), (Forest et al. 2004).

2 ROAD DIAGNOSTICS

Horn antennas which are placed 300 - 500 mm above the pavement surface (for continual measurements) are commonly used in Europe and in the USA. Dipole antennas are commonly used in the United Kingdom. The best results are obtained if a dipole antenna is placed directly on the pavement surface (for continual measurements it is placed approximately 30 mm above the pavement surface).

The measurement is carried out locally or continuously. In the case of a continual survey the GPR system is fixed to a special cart or to a measuring car. The survey is carried out at a slow speed (from walking pace up to 25 km/h – mostly dipole antennas) or at a high speed (80 km/h and more – mostly horn antennas). The main advantage of the high speed survey is the fact that you do not need to close a measured road or to limit traffic on the measured section.

One of the first applications of GPR in the field of road diagnostics was for the location of dowel bars/ tie bars in concrete pavements (Utsi & Utsi, 2004) and the determination of pavement layer thicknesses (Al-Qadi et al. 2005). Currently a GPR application in those

areas is used ordinarily because research in this area is so advanced that it enables the interpretation of measured data to a very high standard. GPRs using antennas with frequency ranges in GHz, controllers capable to operate more channels simultaneously, 3D evaluating software, etc., are able to guarantee sufficiently quick data collection and their following evaluation (Fan-nian, 2000).

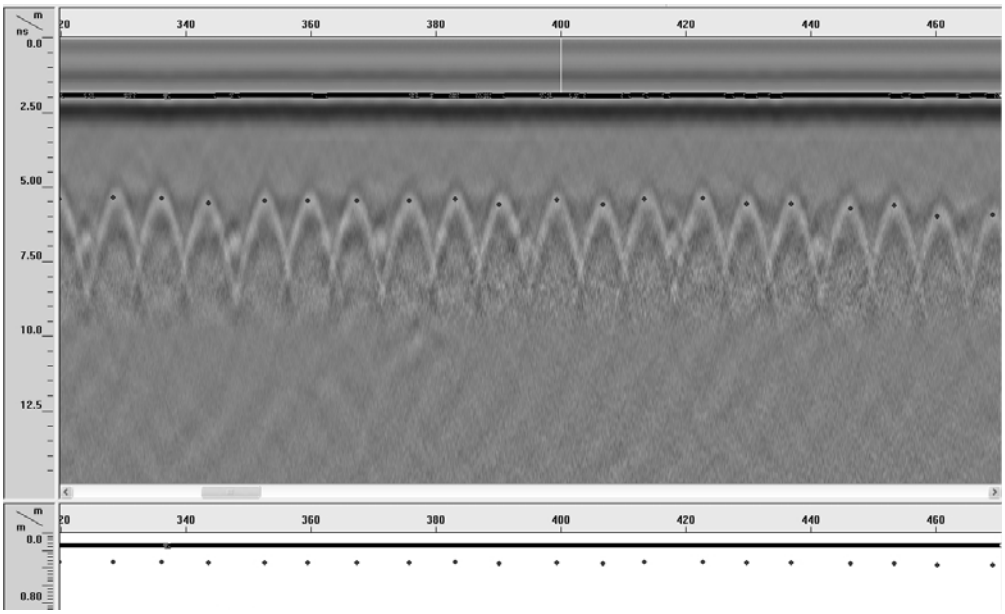

Figure 1: An example of a radargram - location of tie bars in concrete pavement.

Figure 1 presents a radargram from a GPR survey using a 1.0 GHz antenna focused on the location of tie bars in a longitudinal joint of a concrete pavement. This record is further evaluated for determining displacement of tie bars from the center (ideal) location.

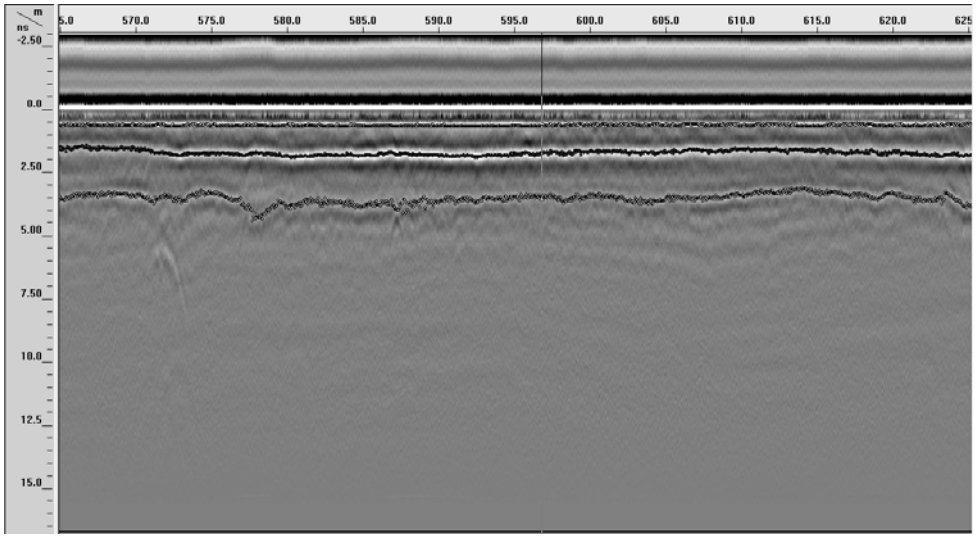

Figure 2: An example of a radargram – the determination of the layer thicknesses of a pavement with asphalt courses

Figure 2 presents a radargram from a GPR survey focused on the determination of construction layers thicknesses of a newly constructed flexible pavement. Surface course, binder course, and base course are marked in colour in the record.

The other contribution to the development of GPR systems was the usage of the antennas' array. On the basis of its usage it is possible to carry out an auto calibration of layer depth measurements. The main advantage is a minimization of the needed cores along the investigated area (Green, 2006).

During the high speed measurement it is possible to locate bigger defects. The smaller defects can be detected but you have to use a lower measurement speed. The main disadvantage of slow speed measurements is a limitation of traffic and the need for road closures.

3 MEASURING DEVICES IN CDV

CDV uses an American system GSSI for GPR measurements in the following two versions:

- The configuration RoadScan 1.0 GHz mounted on a Volkswagen van for measurements at speeds up to 80 km/h (evaluation unit SIR-20, horn antenna 1.0 GHz, supporting frame with treads for calibration, distance indicator located on a back wheel of the vehicle and a calibration plate), see Figure 3.
- A cart for measuring the location of dowel bars and anchors produced and completed at the TRC (the cart, assessment unit SIR-20, two antennas 1.6 GHz of a dipole type, a distance indicator mounted on a separate wheel and a power supply), see Figure 4.

Figure 3: Configuration RoadScan 1.0 GHz mounted on a measuring vehicle.

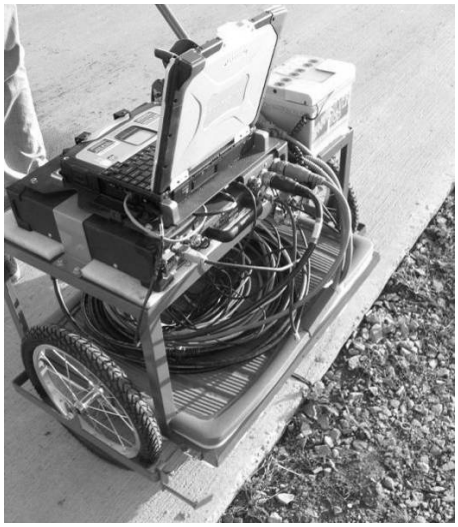

Figure 4: CDV cart with two antennas 1.6 GHz.

4 PREPARATION FOR THE DIAGNOSTICS OF CONCRETE PAVEMENTS USING GPR

The main principle of this preparation was to detect and correctly localize the location of reinforcement. In the standard ČSN 73 6123-1 Road building – Concrete pavements – Part 1: Construction and conformity assessment the following maximum allowed differences between actual location of dowel bars and location designed at the documentation are defined:

a) 20 mm towards the upper slab surface (in the vertical direction),
b) 20 mm towards the longitudinal axis of the concrete pavement (in the horizontal direction),
c) 50 mm towards a transverse joint of a cement concrete surface course (shift in longitudinal direction).

The aim of the experiment was to determine the accuracy we are able to determine the location of dowel bars in a concrete pavement.

A concrete slab with 3 inbuilt dowel bars was produced. The first dowel bar (A) was placed at an ideal location without any shift in either horizontal or vertical direction. The second dowel bar was shifted within the frame of tolerable limits set in ČSN 73 6123-1 and the last dowel bar was located outside the range of these limits.

First, a calibration of the manual cart for distance measurements and GPR calibration by a metal plate located on the surface of the slab was made. Seven crossing measurements of the slab in the direction perpendicular to the location of dowel bars were performed at various distances. During the measurements the perpendicular distances from the antenna to the slab edge were read in two directions, x and y, at the beginning and at the end of the measurement. Performed measurements were evaluated in the program RADAN. The determined location of dowel bars using a GPR was compared with their actual location (see Figure 5).

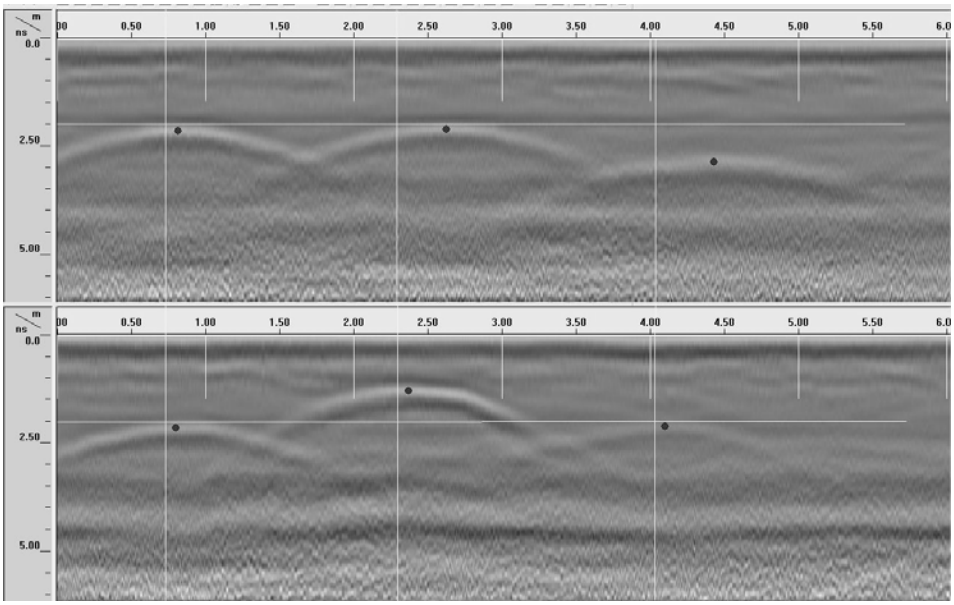

Figure 5: Evaluation of the location of dowel bars in a concrete slab using the program RADAN, comparison of two crossings with a distance 400 mm with visible differences (the dowel bar location is always on the top of displayed parabola).

On the basis of the results of this experiment we concluded that, first, it is necessary to pay attention to the correct location of the antenna at the measurement in order to maintain the accuracy of the measurement in the horizontal direction +/- 5 mm. In the vertical direction the measurement was performed with average accuracy +/- 3 mm. Here we must be reminded that this accuracy was attained using the fact that the thickness of the slab was known and constant all over the slab area. Further, it showed that at the measurements carried out near the ends of the bars are less readable (the parabola is less visible and the accuracy of the measurement is lower).

5 LOCATION OF DOWEL BARS AND TIE BARS

After laboratory tests in situ measurements were performed. For the purpose of measuring the reinforcement of the longitudinal and transversal joints of the concrete pavement a section on the motorway D1 was chosen.

In the transversal direction measurements across the whole profile of the motorway were performed. In the longitudinal direction the measurements were performed on 70 meters of the length. The axial distance of two 1.6 GHz antennas was set to 300 mm. By parallel use of two antennas of the same type and frequency higher accuracy for determining dowel bars displacement was assured rather than if only one antenna had been used and measurement had been performed twice, once at the left side of the joint, and once at the right side of the joint.

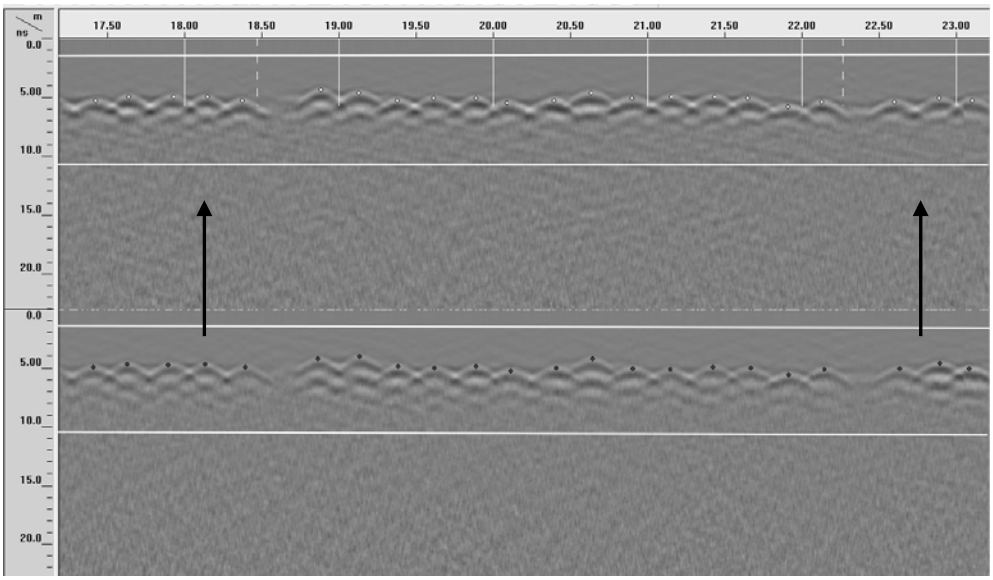

Figure 6: An example of a radargram - location and displacement of dowel bars.

Figure 6 presents an example of the evaluation of the location of dowel bars in the program RADAN. The length of the record is 6 meters. The radargram is divided into two parts which demonstrate data records from two channels, each of which represents a measurement on another side of a transversal joint. The location of dowel bars is represented by the tops of parabolas marked with a point; white lines represent the surface and the bottom of the slab, and a boundary between particular slabs is marked by an arrow.

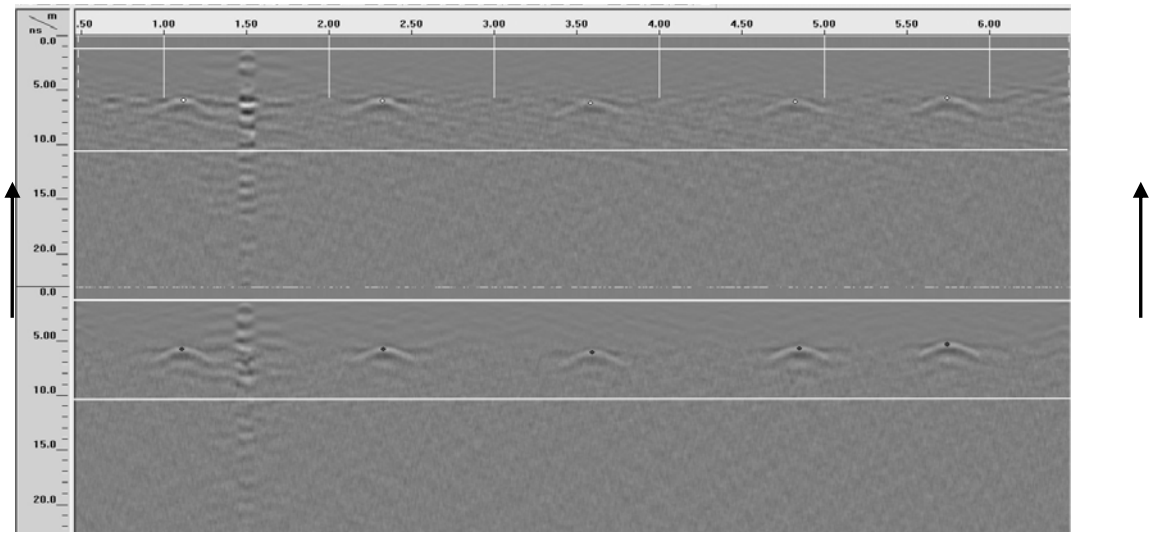

Figure 7: An example of a radargram - location and displacement of tie bars.

Figure 7 presents an example of the evaluation of the location of tie bars in the program RADAN. The record length is also 6 meters long. The interruption of the radargram

at the location 1.5 meter corresponds to the calibration plate which was placed on the pavement surface.

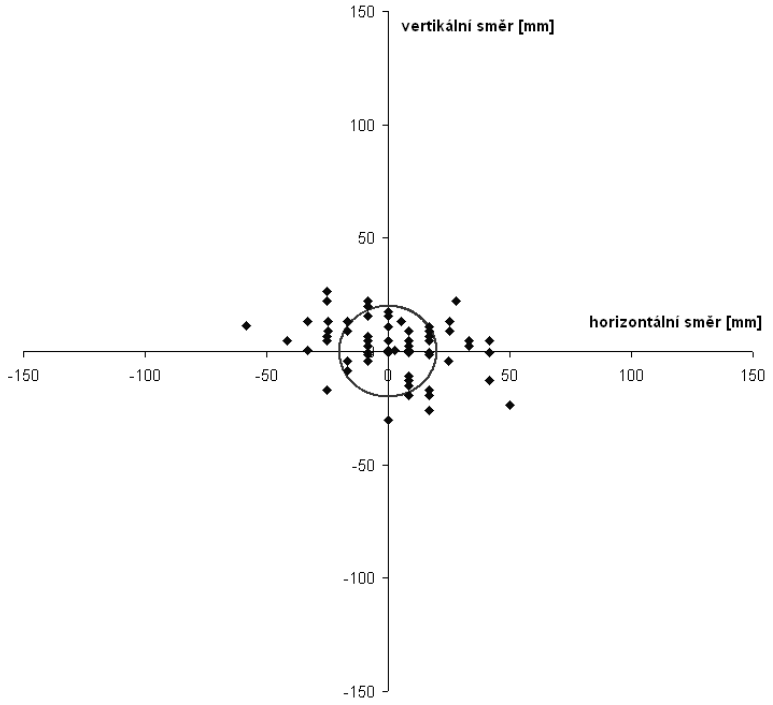

Figure 8: Locations of ends of dowel bars towards the center (ideal) location and their horizontal and vertical displacement.

Figure 8 summarises the location of the ends of measured dowel bars towards the center (ideal) location and their horizontal and vertical displacement in a concrete pavement of 300 mm thickness. The circle marks the boundary location of the ends of dowel bars according to the ČSN 73 6123-1.

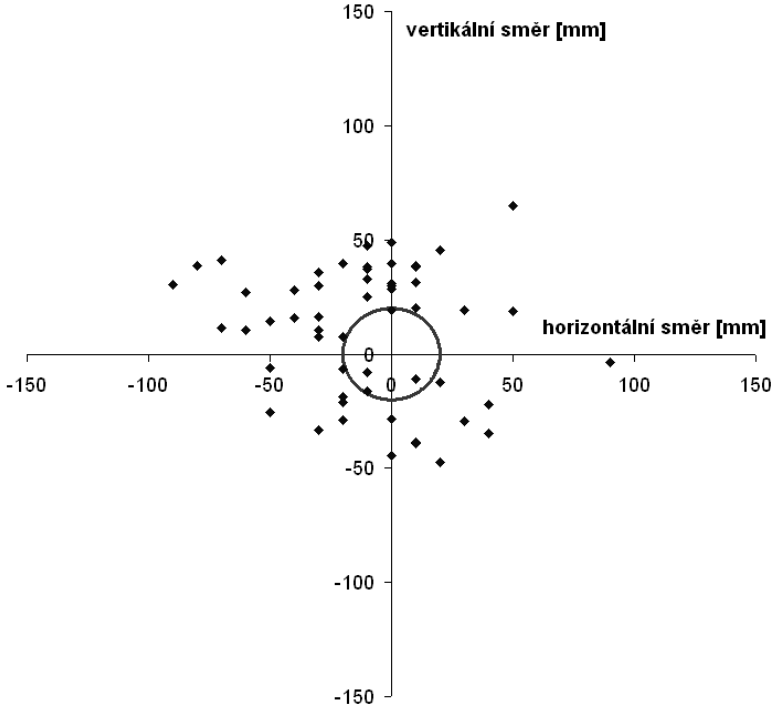

Figure 9: Locations of the ends of tie bars towards the center (ideal) location and their horizontal and vertical displacement.

Figure 9 presents the location of the ends of tie bars towards the center (ideal) location and their horizontal and vertical displacement in a concrete pavement of 300 mm thickness. The circle marks the boundary location of the ends of tie bars according to the ČSN73 6123-1.

It is apparent that even if the boundary location is widened by the measurement accuracy some dowel bars and quite a lot of tie bars will be standing outside the defined limits on the surveyed sections.

Other information concerning GPR testing in general and NDT testing carried out in CDV can be found in (Stryk & Pospíšil, 2006), (Stryk, 2007), (Kořenská, Pazdera et al. 2005) and (Štulířová & Pospíšil, 2008).

6 CONCLUSIONS

The high accuracy of the measurements of the location of dowel bars and tie bars in the horizontal and vertical directions were attained during laboratory measurements.

During in situ measurements the accuracy is decreased because of varied causes, e.g., the change of concrete quality on various sections which can influence the speed of electromagnetic signal propagation in this environment. It is therefore necessary to monitor the slab thickness in order to exclude the influence of these changes in the case of recording an extreme displacement of location of dowel bars and tie bars. It is optimal to determine the thickness of a concrete pavement by one or more cores.

Another influence is the speed of the measurement and the corresponding settings of sampling. It is optimal to perform measurements with a CDV cart at a walking speed. Use of the cart with two antennas enables one to assess the displacement of the dowel bars and tie bars in horizontal and vertical directions.

REFERENCES

Al-Qadi I. L., Lahouar S., Loulizi A.: Successful Application of GPR for Quality Assurance/Quality Control of New Pavements. In: *82th Annual Meeting of Transportation Research Board*, January 12-16, 2003, Washington, D.C., CD-ROM.

Al-Qadi I. L., Lahouar S., Jiang K., MeGhee K. K., Mokarem D.: Validation of Ground Penetration Radar Accuracy for Estimating Pavement Layer Thicknesses. In: *84th Annual Meeting of Transportation Research Board*, January 9-13, 2005, Washington, D.C.,CD-ROM.

ČSN 73 6123-1 Stavba vozovek – Cementobetonové kryty – Část 1: Provádění a kontrola shody (Road building – Concrete pavements – Part 1: Construction and conformity assessment), 2006

Fan-nian Kong.: Choice of Antenna Type and Frequency Range for Testing of Concrete Structures. In: *8th International Conference on Ground Penetrating Radar*, 22-26 May, 2000, Gold Coast, Australia, CD-ROM.

Fauchard C., Dérobert X., Côte Ph. GPR Performances on Road Test Site. In: *8th International Conference on Ground Penetrating Radar*, 22-26 May, 2000, Gold Coast, Australia, CD-ROM.

Forest R., Pynn J., Alani A., Ferne B. *The Use of Ground Penetrating Radar for the Monitoring of Road Properties*. In: *TRL annual research review 2003*. Crowthorne: TRL, 2004, pp. 25-37.

Green R., Lund A., Birken R.: Generation of Utility Mapping Data via Processing of Multi-Channel Signals Collected by Arrays of GPR and EM Antennae. In: *85th Annual Meeting of Transportation Research Board*, January 22-26, 2006, Washington, D.C., CD-ROM.

Kořenská, M., Pazdera, L., Pospíšil, K. et. al. Detection of the Reinforcement Corrosion in Prestressed Concrete Girders. In *8th International Conference of the Slovenian Society for Non-destructive Testing: conference proceedings*, Portorož (Slovinsko), 1.-3.10.2005. Portorož (Slovinsko) 2005, pp. 317 - 322. ISBN 961-90610-5-5.

Stryk J., Pospíšil K. Current possibilities of GPR usage in the field of transport infrastructure. In *4th International Scientific Conference Challenges in Transport and Communications - conference proceedings*, Pardubice, 14.-15.9. 2006 [CD-ROM]. Pardubice : Univerzita Pardubice, 2006, 6 pages, ISBN 80-7194-880-2.

Stryk, J. Road Diagnostics - Ground Penetrating Radar Possibilities. In *Fifth International Symposium Highway and Bridge Engineering 2007* : *proceedings*, Iaşi, România, 7. 12. 2007. Iaşi: Matei - Teiu Botez, 2007, pp. 18 -27, ISBN 978-973-8955-29-5.

Štulířová, J., Pospíšil, K. Observation of Bitumen Microstructure Changes using Scanning Electron Microscopy. *Road Materials and Pavement Design*, 2008, Vol. 9, No. 4, pp.745-754. ISBN 1468-0629.

Utsi V., Utsi E.: Measurement of Reinforcement Bar Depths and Diameters in Concrete. In: *10th International Conference on Ground Penetrating Radar*, 21-24 June, 2004, Delft, pp. 659-662.

Durability of Concrete as a Function of the Properties of the Concrete Layer

J. Adámek
Department of Building Testing, Faculty of Civil Engineering, Brno University of Technology, Czech Republic
**Corresponding author: adamek.j@fce.vutbr.cz*

V. Juránková
Department of Physics, Faculty of Civil Engineering, Brno University of Technology, Czech Republic

ABSTRACT. The changes that the properties of construction materials undergo during this period are extremely difficult to keep track of, and the same holds for the assessment of the causes their degradation. One of the current diagnostic methods to evaluate the actual state of the concrete surface layers is the structure air permeability method. The method was developed theoretically by J.R.Torrent, who also assisted in the manufacturing of an excellent device, the TPT (torrent Permeability Tester). It is a relatively new, non-destructive method, applicable both in the laboratory and on construction sites. This paper will describe the test results from application of different admixture on the air permeability of concrete surface layers.

KEYWORDS: Concrete, air permeability, moisture, durability.

1 INTRODUCTION

Concrete is a heterogeneous material consisting of aggregates bound with cement paste. Its performance properties are thus influenced by the properties of its constituent materials, itsmixing, placement and curing, and its environmental exposure. It is an established fact that differences in relative humidity and temperature in both the curing and storage conditions result in noticeable variations in concrete properties due to the fact that environmental exposure determines the moisture content and moisture distribution in a concrete specimen. Thus, the determination of the moisture content of test specimens at the time of testing is vital for the correct interpretation of test results.

It has been generally understood that in the study of the durability properties of concrete, the topmost concrete cover, which is about 30-50 mm, requires more attention than the inner section, since nearly all transport mechanisms in concrete are influenced by the quality of this layer. Consequently, the gas permeability measurement of concrete cover is considered to be more suitable in assessing the performance properties of concrete than diffusivity, sorptivity or water permeability measurements for various reasons: *e.g.* gas permeability values are more sensitive to changes in the pore structure; gas permeability measurements are relatively simple, take only a short time, and produce repeatable test results. In this respect, the tendencies of current research work are aimed at relating measured gas

permeability coefficients of concrete to the performance properties of concrete in order to make a prognosis of durability (RILEM REPORT 12,1995).

Despite the existence of numerous gas permeability test methods, there is still a lack of general agreement in standardizing. Gas permeability test methods are destructive and suitable primarily under laboratory conditions. In most cases, they require the conditioning of the test specimens before testing and, therefore, test results do not represent the actual situation. For instance, drying concrete in an oven at a temperature of over 100°C results in micro-cracks, while complete saturation results in changes in the pore structure of the testing specimens, due to possible rehydration. Therefore, it is difficult to compare the gas permeability of concrete if not given adequate attention. Instead of test specimen conditioning, the best alternative should be to assess or determine the moisture content of test specimen conditioning just before gas permeability testing, for instance by measuring the relative humidity in the cover concrete and considering the measured relative humidity value in the analysis of gas permeability coefficients. If proper relative humidity measurement methods are incorporated such steps are believed to reduce the effort involved in conditioning specimens in the laboratory and to give the actual material property (Dinku & Reinhardt, 1997).

One of the recent diagnostic methods evaluating the actual state of covercrete porous structure is the air permeability method by Dr. Torrent. The method enables one to quantify the state of covercrete porous structure (into 30-50mm depth) so that from the measured values of the vacuum, which was formed in this covercrete, one can calculate a value of the coefficient of the air permeability k_T and the depth of the vacuum action L. Based on the extensive measurements with TPT (Torrent Permeability Tester), both in a laboratory and "in situ", an author of the testing devices has set a five-degree scale enabling the sorting of the tests of concrete, from a durability viewpoint, into five individual classes from the design values k_T (Torrent, 1992), (Torrent & Frenzen, 1995)

2 THE POSSIBILITIES OF CONCRETE COVER LAYER (COVERCRETE) PERMEABILITY REDUCTION

The deterioration of concrete begins almost after casting, as the hardened properties are influenced by effects which occur at an early stage, such as plastic crashing, segregation and thermal events. Modern design and construction practice has led to improvements. There are two principle methods for improving the covercrete porous structure from the point of view of its impermeability. At first, the addition of different admixtures and ingredients into fresh concrete, and second, to implement the changes in production technology leading to a better quality of concrete from the durability viewpoint. From the admixtures that can modify the porous system of covercrete it is possible to apply silica fume, fly ashes, blast furnace slag, and very fine stone dust. As an admixture, soft polypropylene low modular fibers and high-strength fibers for the spatial reinforcing of concrete can also be considered. The purpose of the application of all admixtures is to reduce the development of cracks in every stage of concrete setting and hardening. The admixtures of hydraulic or hidden-hydraulic character fill the gaps of aggregates used and compress a space on the interface of cement stone and aggregate grain.

The next method for decreasing covercrete permeability is the change of manufacturing technology of concrete. It consists of the selection of cement, design of optimal composition of fresh concrete, and subsequent manufacturing technology and in the placing and curing of fresh concrete. All changes have to be carried out so as to eliminate crack development due to hydration, heat, plastic settlement, and shrinkage in the phase of concrete setting

and hardening, and small cracks caused by gas welding. The cracks originate due to the action of chemical shrinkage and internal drying. Another source of covercrete permeability decreasing are the cracks caused by concrete drying.

The processes leading to the limitation of the development of cracks in a covercrete consist of the selection of cement with a low hydration heat, in restriction of the hydration heat effects, e.g. by overnight casting, in the selection of high-quality aggregates without clay admixture, in the optimal design of fresh concrete composition, in the reduction of water coefficient at attaining the required workability of fresh concrete. Concrete should be placed into quality form work equipped with special covering drainage textiles that reduce the value v/c. Casting in large volumes should be also reduced and the fresh setting of concrete should be treated with water in the course of its maturation. Optionally, it is possible to apply some impervious coating or protective foil for hardening concrete [5] [6]. (Adámek & Juránková, 2003), (Adámek & Juránková, 2003).

3 TORRENT PERMEABILITY TESTER (TPT)

The Torrent permeability tester (TPT) produced by a Swiss company, Proceq, was used for experimental tests on the air permeability of building materials' surface layers, especially that of concrete. The TPT is a modern device, which is applicable for the non-destructive determination of the covercrete air permeability. The device works together with a vacuum pump. The basic parts of the device are two chambered vacuum cells and a pressure regulator that regulates the air flowing into the internal chamber located perpendicular to the concrete surface. Further components of the measuring device are the vacuum pump, regulating unit, and an indicator with an LC display permitting data recording for up to 200 measurements.

The vacuum cell is fixed on the measured area and the vacuum pump is turned on. After about one minute the required vacuum level is reached and the vacuum from the pump works from this moment in the external chamber only in order to balance the pressure in the internal and external chambers. Thus, the air acting around the internal chamber compass prevents an increasing of the pressure in the internal chamber. The indicator records the pressure increasing inside the internal chamber by the air passing through a surface layer into the internal chamber. The air permeability factor of a cylindrical concrete tubus below the internal chamber is derived from Poisseuille`s relation as

$$\frac{dV}{dt} = \frac{kA(P_a^2 - P_I^2)}{2\mu L P_I} \tag{1}$$

where:

V is volume of air penetrating into the internal chamber in the course of time dt

k is air permeability factor (m^2)

P_a is atmospheric pressure (Nm^{-2})

P_I is pressure inside the internal chamber (Nm^{-2})

A is cross-sectional area of the internal chamber (m^{-2})

μ is dynamic viscosity of air (Nsm^{-2})

Effective depth $L(t)$ in time t is a depth in which the air inside the pores reached the atmospheric pressure P_a. The pressure changes linearly which the depth. By inserting a set of hypothesis into the relation (1), we obtain the definite relation for permeability factor calculation k_T

$$k_T = 4\left[\frac{V_c\left(dP_I / dt\right)}{A\left(P_a^2 - P_I^2\right)}\right]^2 \frac{\mu P_a}{\varepsilon}\int_{t_o}^{t}\left[1-\left(\frac{P_I}{P_a}\right)^2\right]dt \qquad (2)$$

where:

V_c is volume of the internal chamber and body through which the air flows (m^3)

ε is open porosity of concrete (m^3m^{-3}) and

dP_1/dt is derivation of pressure with time t ($Nm^{-2}s^{-1}$)

The calculation of both constants k_T a L is performed with numeric integration and derivation with software of the indicator. The problem is the determination of the constant ε - open porosity of concrete, which is different for various concretes. This constant is either estimated or determined by tests. For the air permeability factor k_T calculations with the TPT mean value of the open porosity ε = 0.15, that was evaluated by the author of the TPT from the extensive sets of tests, were used (Torrent, 1992).

4 EVALUATION OF CONCRETES FROM THE POINT OF DURABILITY

Based on the extensive experimental research of the author of the device (Torrent, 1992), both in laboratory and in situ, criteria were determined for the evaluation of concrete durability. Classification of the covercrete quality is specified in 5 classes (Table 1). To every quality class a range of values of the permeability factor is assigned determined by the concrete after 28 days aging.

Table 1: Classification of the Quality of the "Covercrete" according to k_T.

Clasification of the covercrete quality		k_T measured at 28 days [$E^{-16}m^2$]
1	very good	$k_T < 0{,}01$
2	good	$0{,}01 < k_T < 0{,}1$
3	normal	$0{,}1 < k_T < 1{,}0$
4	bad	$1{,}0 < k_T < 10$
5	very bad	$k_T > 10$

The permeability factors k_T are valid for dry matured concretes. When concretes are wet, or there are doubts whether they are dry or wet, the Wenners four points probe, that measures

electric resistance ρ [k ohm cm], is used. The value of resistance ρ is measured prior to the determination of the permeability factor k_T, or optionally the mean value ρ is inserted into the indicator manually. The amount of water or vapor in a porous structure of concrete significantly influences the concrete's extent of permeability. The more wet the concrete is, the less is its permeability, and it appears to be of high performance from the viewpoint of durability. After water has evaporated from the pores, the permeability value increases and concrete is more permeable.

5 EXPERIMENTAL WORKS

5.1 Silica fumes as an admixture into concrete

We tested the influence of powder silica Sioxid and micro-silica in a water suspension Elkem on the values of the coefficient of permeability to air k_T. The compared reference without silica was measured, (R). The doses were identical for both types of admixture, 5 and 10 %, from the weight of cement (B-E).

The admixtures in both doses have an impact on the bending strength. The increase was about 17% higher. The compressive strength of concrete was almost the same. The comparison of permeability coefficient k_T in all concretes in relation to moisture is shown in Figure1.

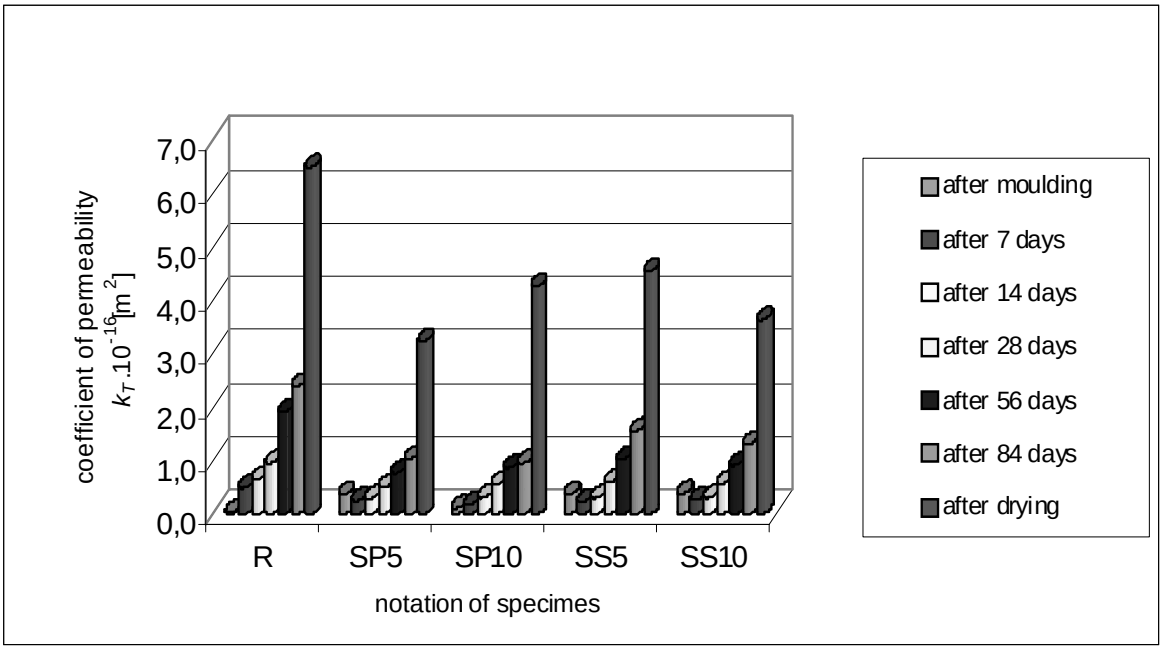

Figure 1: The relation of permeability coefficients on aging in silica concrete fume.

5.2 Fly ash as a part replacement of fine aggregate

Fly ashes and blast furnace slag performed similarly as silica fumes. Both materials create a soft part of fresh concrete and improve its plasticity, compress the contact zone

among the aggregate grains and matured cement. Hydraulicity of both components contributes, not only to the "sealing" of a concrete structure, but especially to the tensile and compressive strength enlargement. Last, but not least, they contribute to the decreasing of the concrete's permeability to liquids and gases, and thus to the improvement of covercrete property in the durability viewpoint.

5.3 Fibers as reinforcement for cracks reduction

Polymer soft fibers were dosed into fresh concrete in a volume of 0.6 and 0.9 kg/m^3 in accordance with the producers' recommendations. The basic properties of 4 different concretes with PP fibers (B-E) and comparative concrete without fibers (A) were verified. Even though it was not assumed that these soft fibers would contribute to strength improvement, the bending strengths tested at ages 7, 28 and 84 days were on average about 13.5 % higher than comparative concrete. The effect of the improved state of covercretes with fibers (in Figure 2 and 3 marked B-E) reveal curves expressing the influence of the values of the coefficient of permeability for air k_T on the aging period and on the moisture of tested concretes. In both cases the values k_T of concrete B-E were lower than ones of comparative concrete. The water content in the porous layer of the tested concretes principally influences the real values of permeability.

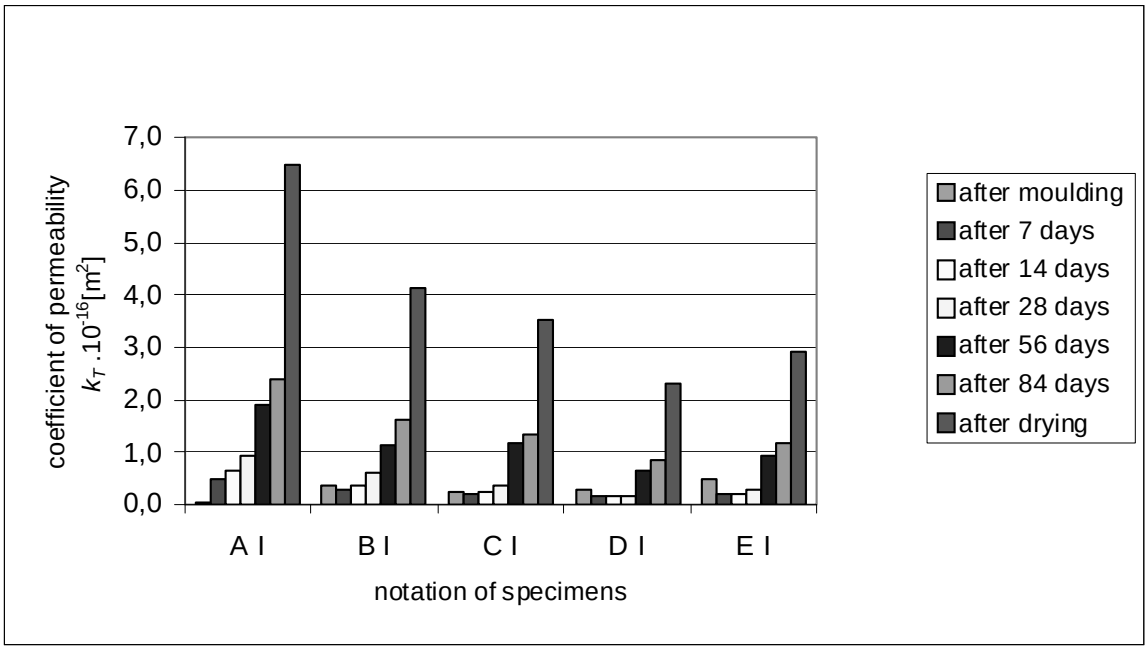

Figure 2: Coefficient of permeability k_T in relation to aging time in concrete with soft fibers.

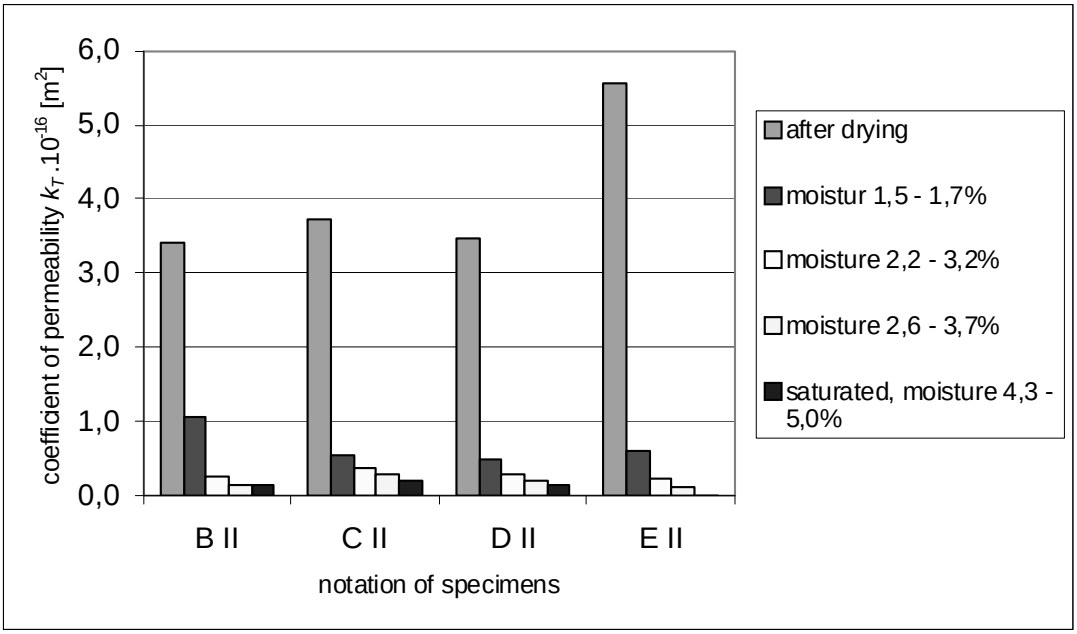

Figure 3: The relations of permeability coefficients and moisture content in concrete with soft fibers

6 CONCLUSION

The objective of this contribution was a recapitulation of the possibilities of covercrete impermeability improvement and, by that, to specify the procedures on how to reduce an intrusion of aggressive gaseous and liquid media into concrete. The methods consist of the design of concrete mixtures, or in the change of the manufacturing technology of concrete, and demonstrate in a different way the properties improvement of hardening concrete in relation to its durability.

7 ACKNOWLEDGMENT.

This paper presents results of research supported by the project of GAČR 103/09/0065 and project VVZ MSM 0021630511.

REFERENCES

Adámek,J., Juránková, V.,2003 *Permeability of Concrete with PP-Fibres,* Int. Symposium F. bre Concrete and High-performance Concrete, Malenovice, Czech Republic, pp. 136-143.

Adámek,J., Juránková,V.,2003, *Air Permeability of Concrete,* IV. Konferencija Naukowo – Techniczno, Zagadnenia Materialowe w Inżynierii Ladowei, Krakow, Polsko, pp.43-49.

Dinku,A., Reinhardt,H.W, 1997, *Gas Coefficient of Cover Concrete as a Performance Control,* Materials and Structures, Vol.30, pp.387-393.

RILEM Report 12, 1995, *Performance Criteria for Concrete Durability*, TC 116-PCD, Performance of Concrete as a Criterion of its Durability, Ed. Kropp,J., Hilsdorf, H.K, 1995 (E+FN Spon).

Torrent,R.J., 1992, *A two-Chambers Vacuum Cell for Measuring the Coefficient of Permeability to Air of the Concrete Cover in Site*, Materials and Structures, vol.25, pp.358-365.

Torrent,R.J., Frenzer,G.,1995, *A method for the rapid determination of the coefficient of permeability of the "covercrete"*, Int. Symposium Non-destructive Testing in Civil Engineering (NDT-CE), Berlin, p.985-992.

Experimental Testing of the Applicability of Betatrons in Construction Radiography

O. Anton* & V. Heřmánková
Brno University of Technology, Faculty of Civil Engineering, Brno, Czech Republic
** Corresponding author: anton.o@fce.vutbr.cz*

ABSTRACT: This paper focuses on testing the possibility of using portable betatrons in the radiography of reinforced concrete structures of greater thicknesses. The experiments were carried out in cooperation with the Research Institute of Introscopy in Tomsk (Russia).

KEY WORDS: Radiography, reinforced concrete, betatron.

1 INTRODUCTION

The properties of reinforced concrete structures with thicknesses of up to 0.6 m are tested by various non-destructive and destructive testing methods. However, for greater thicknesses of reinforced concrete structures, such as concrete bridge piers, massive foundations for rotating machines, and also massive shielding structures of linear accelerators and particularly of nuclear power plants, the standard methods often fail.

This was the reason for proposing a radiographic control method, which was then successfully tested, using a portable radiation source with the highest energy of breaking radiation so far - betatron MIB-7.5 MeV, which enables one to irradiate reinforced concrete structures and determine their macrostructure up to a thickness of 1 m. Experimental irradiation of concrete samples with embedded reinforcement was carried out at the Research Institute of Introscopy in Tomsk (Russia).

2 APPLICATION AREA OF BETATRONS

Ionizing radiation sources with the energy of particles from 1 to 30 MeV are applied in various areas of human activity. These are mostly the non-destructive testing (NDT) of materials and products, the evaluation of the inner contents of various objects without damaging them (control), and applications in health care.

Radioactive isotopes and various types of accelerators, such as betatrons, microtrons and linear accelerators, are now used in the above mentioned fields as the sources of ionizing radiation.

A betatron is a cyclic induction electron accelerator, where the energy of particles increases due to the eddy-current electric field, i.e. by changing the magnetic flux through the particle orbit. A betatron is the simplest accelerator, but it is inferior when compared

to other types of contemporary accelerators. These properties determine the advantages and disadvantages of betatrons.

The first working betatron was assembled by D. Kerst in the USA in 1940. The first betatron in Russia was put into operation at the Tomsk Polytechnic University (TPU) towards the end of 1946.

The Research Institute of Introscopy (RII) was founded in 1968, at first as a designing department of the Tomsk Polytechnic University. Later on it gained total independence and now it has the status of a federal state research institution subordinate to the Ministry of Education and Science. On the grounds of the policy of reduction, the RII was again transferred under the jurisdiction of the Tomsk Polytechnic University on the basis of Russian Government regulation.

In the 1950s and 1960s, a number of countries produced betatrons with energies from 15 to 45 MeV for use in non-destructive testing and health care. These were the so-called primary units, which were rather big and heavy. Later on, due to the quick development of microwave technology, these betatrons were replaced with linear accelerators able to provide 10 to 100 times higher dose rates.

Today, only the so-called "small-size betatrons" are required, the size and weight of which enables their transport to the objects tested. In the 1960s, the TPU started production of these small-size betatrons for energies from 3 to 6 MeV for use in non-destructive testing under non-stationary conditions. Since the 1980s, the production of small-size betatrons has been one of the major tasks of the Research Institute of Introscopy. The Institute has become almost the only supplier of these devices for technological usage within Europe.

Small-size betatrons as the sources of radiation for non-destructive testing have a lot of advantages in comparison with other types of accelerators and radionuclide radiation sources. They have a slightly higher energy of radiation, small size of focus, the possibility of setting a maximum energy, a continuous range of breaking radiation. These properties enable the use of one unit for examining materials and products of a wide range of thicknesses. Apart from that, the issues of radiation safety are handled much more easily for small-size betatrons in comparison with the radionuclide sources.

However, as far as the acceleration principle used is concerned, standard betatrons do not allow for the acceleration of a higher number of electrons during one cycle, and this results in a lower dose rate when compared to other accelerators. That is why betatron designers primarily focus on increasing the dose rate. The latest models of small-size betatrons have had the dose rate increased 15 to 20 times when compared to the first samples; the size and weight have remained the same. Good radiation characteristics, simplicity and output reliability, as well as radiation safety in the OFF state ensure a sustainable demand for small-size betatrons, both in Russia and abroad. This demand consists in the price of a small-size betatron, which is several times lower than the price of a linear accelerator with the same energies.

Small-size betatrons produced nowadays in the Research Institute of Introscopy can be divided into the following groups:

1. Small-size betatrons for the non-destructive testing of materials and products. Most betatrons in this group can be used under non-stationary conditions.
2. Small-size betatrons of the control systems, including customs controls in applications for large containers, products and luggage.
3. Small-size betatrons with an extracted electron beam for medical purposes and radiation tests of electron products.

The following technical solutions offering an effective application of betatrons and easy operation were implemented for the betatrons of the first group:

- setting up energy in a large range, which enables the checking of various thicknesses with a maximum speed
- using one's own dosimetric devices, consisting of a dosimeter placed behind the tested object and of a built-in dosimeter measuring the output dose. This allows one to skip experimental exposures completely and improve the quality of films;
- fully automatic control by microprocessor systems carrying out the setup and stabilization of all the parameters of the accelerator, switching off the source of radiation after achieving the preset dose on the basis of information in the built-in dosimeter, as well as on the basis of the time signal. Thus, the only thing the operator must do is to press the button triggering the radiation;
- small sizes and weights, which allows one to use most types of small-size betatrons under non-stationary conditions.
- setting the repeat frequency of radiation impulses to reduce consumption, which facilitates work under field conditions using low-energy sources.

Technical characteristics of betatrons used today in non-destructive testing are summarized in Table 1.

Table 1: Technical characteristics of contemporary betatrons.

Number	Characteristic	Model				
		MIB-3.5 „Axis“	Betatron „TOMO“ (for tomography)	MIB-6 (PXB-6)	MIB-7.5 (MXB-7.5)	MIB-10 (KRAB)
1	Energy setup range, MeV	2 to 3.5	3 to 5	2 to 6	2 to 7.5	3 to 10
2	Dose rate at 1 m from the target point in the peak, R/min	2.7	4	3	5	20
3	Sizes of foci mm x mm	0,3x3	0,3x3	0.3x3	0.3x3	0.3x3
4	Maximum PRR, C-1	400	400	200	200	150
5	Maximum thickness of steel for attenuation, mm	150	150	200	250	350
6	Unit weight: kg Source of radiation	55	500 (shielding)	97	105	275
	Feeding	56	35	51	63	80
	Control Panel	1.0	1.0	1.0	1.0	1.7
7	Energy consumption at the max. frequency, kW	2.2	2.5	2.0	2.5	3.6

Betatron MIB-7.5 is the most commonly used product today.

At the moment, there is no information available that betatrons, including small-size betatrons, would be manufactured by any other organization than RII.

So far, however, the use of betatrons has, in fact, been limited to radiography in mechanical engineering, i.e. irradiation of massive metal elements. This is why we have established a partnership with the Research Institute of Introscopy, with the aim to test the actual possibilities of using their most perspective model of betatron MIB-7.5 for the irradiation of higher thicknesses of reinforced concrete.

3 PRINCIPLE AND DESCRIPTION OF BETATRON

A betatron is a cyclic induction electron accelerator producing high-energy radiation, the so-called breaking radiation, as a result of a conversion of kinetic energy of electrons during their collisions with the target. Electrons are accelerated by the eddy-current electric field, i.e. by changing the magnetic flux on the closed particle orbits. The alternating magnetic field is induced in the electromagnet of betatron by means of magnetic coils and profiled pole pieces, around which there is a toroidal vacuum accelerator chamber.

A betatron consists of three main units: the source of radiation, the power unit, the control panel and two additional units – the stand-alone dosimeter and the light alarm unit that are used as needed. The scheme of betatron MIB-7.5 is shown in Fig. 1.

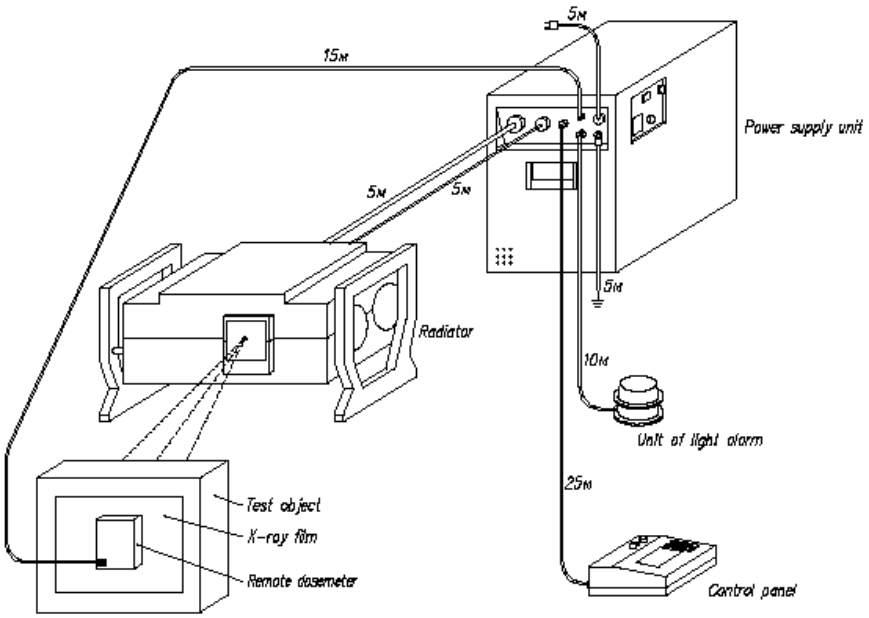

Figure1: Betatron MIB-7.5.

4 BETATRON MIB-7.5 BASIC DATA FOR THE RADIOGRAPHY OF CONCRETE

Betatron MIB-7.5 is recommended for the irradiation of building constructions made of concrete or other materials with a thickness from 200 to 900 mm. The limiting thickness for concrete is 1200 mm, and it is limited by the exposure time. The maximum exposure time is determined by the time when betatron can be in operation in one cycle. Here, therefore, we can see a limitation in comparison with the radioactive sources.

The breaking radiation of betatron has a continuous energy spectrum and theoretically it contains quanta of photons in the extent from the maximum value (equal to the kinetic

energy of accelerated electrons) to zero. In the case of shielding it is recommended to use the term "effective energy". According to the documentation its value equals a half of the maximum value.

Half-thickness (an important shielding parameter) for energies 7.5 and 5 MeV for concrete is 110 mm and 91 mm.

The main radiation parameters monitored – sensitivity and quality of the film – are defined by the sensitivity and contrast of the radiographic film emulsion and by the type of intensifying foils. Intensification in metal foils is based on the subsequent influence of electrons on the radiographic film. The foils are made of heavy metals (lead, tungsten, tin, tantalum, etc.). The intensifying effect of the foils depends on the thickness of the front and rear foils, the energy of the radiation, and on some additional factors. Sensitivity depends on a number of factors: energy, focus, the thickness and the shape of the product, film type, intensifying foil, focal distance and the experience of the operators. Quality of the film is monitored by means of wire gauges.

The exposure time of betatron can be set up on the basis of an exposure diagram (Fig. 2) or a built-in dosimeter.

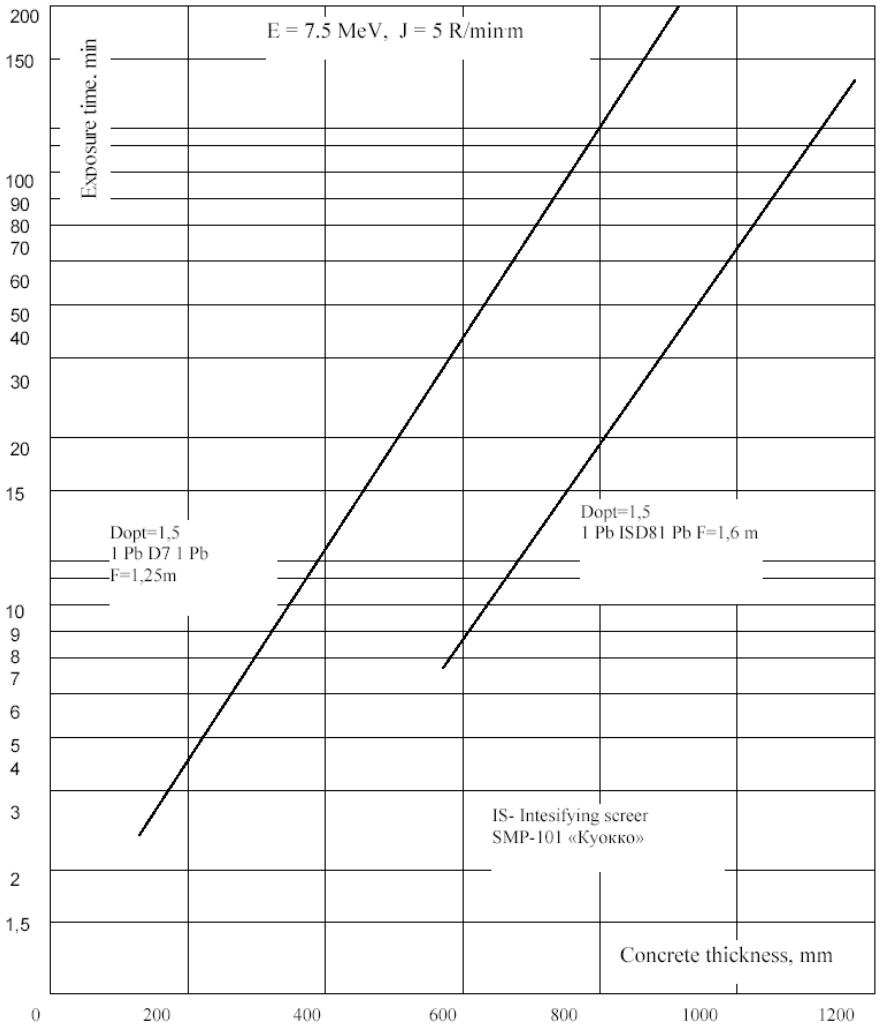

Figure2: Diagram of exposure times for concrete.

5 TESTING THE USE OF BETATRON MIB-7.5 IN THE RADIOGRAPHY OF REINFORCED CONCRETE – EXPERIMENT

The aim of the experimental work was a preliminary determination of the maximum thickness of irradiated concrete and of the sensitivity of imaging using betatron with the energy of 7.5 MeV as the source of radiation.

In the laboratory of the Research Institute of Introscopy in Tomsk, an experimental path was assembled according to the instructions, similar to the one in the laboratory of the Radiation Defectoscopy Centre in Brno.

It consisted of concrete slabs with dimensions of 500 x 500 x 100 mm.

One slab contained rods of steel reinforcement of class 10 216 with diameters of 36, 25, 18 and 10 mm placed horizontally. Unfortunately, irradiation of other types of reinforcement was not agreed with the Centre. The slab with reinforcement was placed second in order; the depth of reinforcement placement was therefore approximately 150 mm.

Figure3: Experimental path in Tomsk, ends of steel reinforcement apparent in the 2nd slab.

What is interesting in this case is the use of wire gauges, which was not a problem thanks to a greater focal distance. The wire gauge was made as the so-called irradiation standard, in accordance with the local practice.

A detailed picture of this standard is shown in Fig. 5. The diameters of individual wires were: 3, 4, 5, 6, 7, 8, 9 and 10 mm, and their length was 100 mm. The gauge was fixed to a fiberglass plate with a thickness of 2 mm. The distance between the wires was 7 mm.

A solid cassette with a radiographic film 30 x 40 cm was placed immediately against the rear edge of the last slab. The film was placed between two steel foils with a thickness of 1 mm (using steel foils for betatron is adequate to lead foils when irradiating with Co-60). All the images were exposed on standard Agfa D7 films.

The spherical chamber of clinical dosimeter 27012 (made in Germany) was placed behind the cassette and into its centre. The exposure was carried out with a view to a possible dose at this dosimeter. At the same time, the exposure time and the dose achieved by the betatron internal dosimeter were registered. It is worth mentioning that the internal dosimeter of betatron is calibrated by clinical dosimeter 27012, the spherical chamber of which is situated on the beam axis at a distance of 1 m from the target. The focal distance between the target of betatron and the cassette was 1.5 m for all images.

On the basis of the previous experiments, the maximum density of blackening was chosen to be D = 3.0. All films were developed manually. The blackening was measured in two sections, in the centre of the image containing no horizontal or vertical rod, and in the lower part of the image along the line close to the edge of the horizontal rod with the highest diameter. Five points were measured and these data were used for determining the average density of blackening.

Table 2: Characteristic parameters of radiograms taken.

Image number	1	2	3	4
Thickness of concrete [mm]	600	700	800	900
Dose behind the film [mGy]	19	18	18	18
Exposure time [min.]	24	52	77	124
Dose of internal dosimeter [Gy]	1.60	3.20	4.72	7.60
Optical density in the image centre	2.64	3.00	2.58	2.37
Optical density in the image margin	1.90	1.96	2.03	1.79
Min. discernible of steel wire [mm]	3	3	3	4

The total exposure time of images 3 and 4 was completed only after a 15 min break in the exposure (after 45 min run) because of a complete cooling of the betatron.

Figure 4: Scheme of the experiment in Tomsk – betatron MIB-7.5 and the experimental path.

During the evaluation of radiograms it was ascertained that all reinforcement rods in all radiograms are unambiguously visible. The quality of radiograms was almost identical regardless of thickness. Also regardless of thickness we can therefore presume the possibility to identify the reinforcement type. In all images it can be estimated that it would be possible to identify the type of reinforcement with diameters of 25 and 36 mm, but not so in the case

of lower diameters. Unfortunately, a comparison with an image of rebar reinforcement was not possible (due to limiting the original scope of tests).

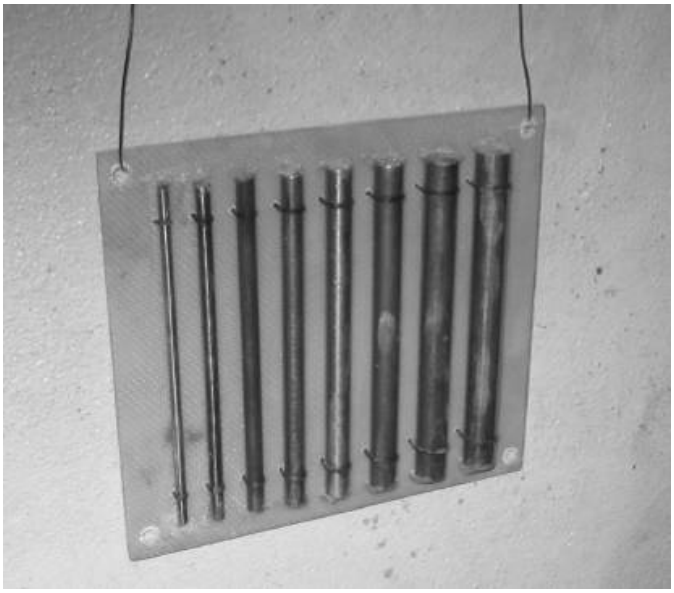

Figure 5: Wire gauge made up of wires with diameters of 3, 4, 5, 6, 7, 8, 9 and 10 mm, in accordance with local standards.

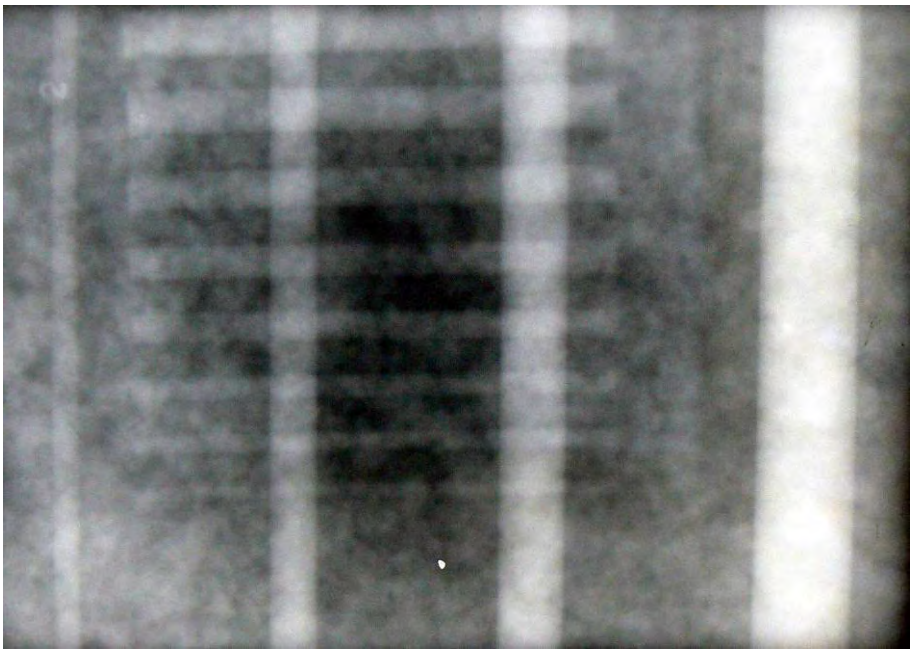

Figure 6: Radiogram at a concrete thickness of 600 mm.

6 RESULTS OF THE EXPERIMENT USING BETATRON MIB-7.5

The experiments carried out do not implement fully all the possibilities of concrete structure testing using betatron MIB-7.5 (it would be possible to increase the irradiated thickness

of concrete even more). In spite of this, we can summarize the conclusions of the experiment in the following points:

- Steel reinforcement rods in the concrete are clearly visible. Even in the worst case, when the reinforcement is close to the edge of the concrete structure and is directed towards the radiation source, the sensitivity was not worse than 0.5%.

- The analysis of radiograms allows us to draw some conclusions about the quality of concrete. Insufficient homogeneity of concrete is clearly visible in all the images. The reason for this is that the concrete blocks used were made manually and the content of concrete fractions was not checked.

- The non-homogeneity of blackening is also well visible, which is caused by the non-homogeneity of the radiation beam of betatron. With a focal distance of 1.5 m and in an image with dimensions of 300 x 400 mm, the non-homogeneity of blackening from the centre to the edge could be 0.6 to 0.7 blackening units on average. This does not visually influence the detectability of the defect too much. In spite of that, for achieving good density imaging in the centre, approximately 3 units of optical density should be optimal.

- Also worth noting is the apparent haze near the rods at a concrete thickness of 800 mm, and especially at a thickness of 900 mm. This is related to a great optical magnification of about 2.5 times at a thickness of 900 mm. This is the reason why the focal distance at a concrete thickness of 800 – 900 mm should be at least 2 m.

- When we use the D7 film with lead foils, the exposure time is too long. Starting with the thickness of 700 mm, it is impossible to get an image within the time corresponding to one betatron cycle. This is the reason why it is necessary to study the effective use of betatron MIB-7.5 in testing great thicknesses of concrete which reduce the exposure times.

According to the description of betatron, if the D8 film is used with a SMP-101 "Kyokko" intensifying foil, it is possible to reduce the exposure time approximately 7 to 8 times, but at the price of lowering the quality of radiograms.

Another possible way of reducing the exposure time is the new methodology of radiographic control: memory foils, scanners for the reading and digitalization of their images and further digital processing for improving the quality of images.

The Research Institute of Introscopy focuses on this issue at the moment. It has recently bought memory foils and HD-CR 35 NDT scanners made by the German company “DŰRR NDT” and software packages Video Ren made by the company “Unitest-Roentgen (St. Petersburg)” for processing images. They are being studied at the moment, but their description indicates neither instructions for use, nor the characteristics of sheets: sensitivity to doses, resolution, etc.

The experiments are in progress at the moment.

As a conclusion it is possible to state that the use of betatron MIB-7.5 in construction radiography is basically possible, and even for the irradiation of higher thicknesses of concrete than Co-60 radiography normally allows. The necessary exposure times are incomparably shorter, but on the other hand, it is necessary to switch off and cool the device between the maximum exposure times, which prolongs and complicates the whole process.

Moreover, due to its size and weight, the device is designated for only exceptional use in the field, in some extraordinary and well-founded cases. This, apart from its high purchase cost, is also the reason why its use has not yet spread widely. At the moment, memory foils are tested, the use of which could shorten the exposure times to values not approaching the boundary exposure times, which could lead to a wider proliferation of the device.

REFERENCES

Anton, O.; Heřmánková, V. *Možnost užití betatronů při radiografii masivních konstrukcí*. In Zkoušení a jakost ve stavebnictví 2009. Brno, VUT v Brně. 2009. p. 49 - 59. ISBN 978-80-214-3951-1.

Luňáček, M.; Anton, O.; Vymazal, T. *Příprava masivních bloků pro projekt „Metodika zkoušení masivních železobetonových konstrukcí“*. In Juniorstav 2007. Brno, VUT v Brně, Fakulta stavební. 2007. p. 166 - 173. ISBN 978-80-214-3337-3.

Technical Notes on GAST Final Days

by Jana Kadlecová - *Faculty of Transportation Sciences, Czech Technical University in Prague, kadlecova@lss.fd.cvut.cz*

November 30th was the final day of the GAST project‘s life. The project, whose full title is Green And Safe Transportation, was financed through the EU – EC, Directorate for Education and Culture. This activity involved 18 highly professional academic and industrial partners from 7 countries and closely cooperated with three other pilot projects aimed at the innovation and improvement of the exchange of knowledge between academic and industrial areas. The importance of this quartet was primarily based on new scenarios that should show possible ways in which to accelerate the advancement of technologies accessible for all subjects needed; not necessarily to create them, but to rather find some working scheme that would enable access to information and improve its usability.

These four pilot projects, comprising of SUCCESS, BRIDGE, EIT, and, of course, GAST cooperated well and aimed at better knowledge management and the support of a “European” knowledge network.

The first task to solve was the choice of the most efficient tools to support the technology and knowledge transfer. Professionals involved in expert teams have come to the consensus to choose four test cases to prove new collaboration models, sustainable for the long-term. These test cases were developed and validated as applicable for real use. Based on the validation, several recommendations were formulated and will be presented to the European Commission as a lead for future regulation proposals.

The test case Project House dealt with the idea of a shared space where universities, industries and public bodies can meet to solve tasks that are a matter of mutual interest. Project House consists of several components that support the applied-oriented scientific activities performed. Project House has to foster innovation and technology transfer, and education and knowledge transfer by different means. The practical application will be launched in Germany and its main aim is to join the forces of universities and industries to develop or improve principles leading to lower/none carbon dioxide emissions.

Other activities that were performed were connected to the area of education, as professionals will be prepared for brand new internationally linked working principles that are a necessary prerequisite for successful future cooperation.

One of these was the Project Workshop, an international workshop of students of different educational origin who gather together in order to solve some specific task. This activity can teach its members how to cooperate using communication tools and to be responsible for teamwork’s result.

The European Automotive Master study programme is a slightly moderated multiple degree study programme that offers the possibility to learn with excellence. Each member university offers the subject matter they are leaders in and there is a board to evaluate the validation of each of the members.

The last case study was aimed at the networking of currently existing separated clusters. This activity is titled Cluster of Clusters and should assure the sustainable cooperation of clusters of similar interest. As an example, the working team states EASN as a network joining clusters and facilitating the flow of knowledge between different European hubs.

As a result, there were some recommendations given for the legislative bodies and probably even for universities that are responsible for the creation and management of their study

programmes, as these need to give the students elementary preparation in order to be able to take part in such activities.

All of the test cases performed showed the need of partial physical co-location and interaction for their long-term workability. This means that for any of the collaborative activities the "meeting" of participants is a key factor for success. Another important enhancement is provided by the good balance of private and public funding, and governance. Governance should mirror the bodies and their interests involved in projects in order for balance to be kept for all members; GAST has applied a four-layer approach.

One of the applications which are already known and that came into existence recently are KICs, which have not completely started operation, but are being prepared for launch at the moment.

What seems to be crucial in any academic-industry co-operation is the person acting as the interface; this person raises the benefits of all involved. On the other hand, the commitment of members in supporting the mutual interest is another key part.

Altogether, along with partner projects, GAST has shown that international cooperation is an inevitable part of future professional work in the automotive industry, either in development or in mass production.

Currently, the EC is taking action leading towards the introduction of new schemes of cooperation within Europe, and hopefully will respect the recommendations resulting from these four activities.

Index of Titles

Volume 2/ 2009

Index of Authors

Volume 2/ 2009

Editorial Apology

ToTS 2/ 2009

Change the order of authors

from:

J. Kovanda, T. Růžička * – *Faculty of Transportation Science, Czech Technical University in Prague, Czech republic*

M. Kepka – *Research Centre of rail Vehicles, Faculty of Mechanical engineering, University of West Bohemia in Pilsen, Czech Republic*

to:

T. Růžička *, J. Kovanda – *Faculty of Transportation Science, Czech Technical University in Prague, Czech Republic*

M. Kepka – *Research Centre of rail Vehicles, Faculty of Mechanical engineering, University of West Bohemia in Pilsen, Czech Republic*

TRANSACTIONS ON TRANSPORT SCIENCES

Volume 2 2009 Number 4

CONTENTS